BMC Chemistry

RESEARCH

Open Access

FTIR spectroscopic studies with thermo acoustical parameters in binary and ternary liquid mixtures of amino acid and saccharide in aqueous medium

Rupesh Kumar Pradhan[1] and Sulochana Singh[1*]

Abstract

The interactions between amino acids and saccharides in aqueous environments are fascinating and have significant implications for various fields. These interactions can provide valuable insights into physiological processes, drug targeting, and delivery systems. To comprehend the synergy between saccharide (L-arabinose/D-xylose) and non-essential amino acid (L-aspartic acid; Asp) in an aqueous system, ultrasonic velocity (*U*) at 293.15 K–313.15 K (with 5 K interval) and at experimental pressure P = 101 kPa were measured using a digital ultrasonic interferometer. The solution density,ρ and the propagation of sound waves through the experimental solutions are directly correlated with the weak and strong molecular interactions that take place between the solution's constituents. ρ and *U* data was utilised to compute the following acoustic parameters isentropic compressibility K_s, apparent molar isentropic compressibility $K_{s,\phi}$, free volume V_f, free length L_f, internal pressure π_i, acoustic impedance Z, surface tension γ and relative association R_A. Positive K_s^0 values make ion–solvent interactions stronger than ion-ion interactions. Positive values of $K^0_{s,\phi,\,tr}$ imply greater interactions between the polar segments of L-arabinose/D-xylose and the zwitterionic groups of Asp. The solvation mechanisms of Asp result in the reconstruction of the water structure. The FTIR technique was used to verify the results of the acoustic study. The presence of intermolecular hydrogen bonding and intramolecular hydrogen bonding is shown by the broadening of the absorption band. The system under research exhibits predominant ion-hydrophilic/hydrophilic interactions as confirmed by FTIR analysis. Understanding how Asp in aqueous environment interacts with saccharides such as L-arabinose and D-xylose might help one better understand how these molecules behave in biological systems.

Highlights

- Acoustic properties were evaluated for Asp in aqueous saccharide solution
- K_s decreases as Asp and saccharide (s) concentrations rise
- In the presence of saccharides, Asp serves as a structure maker
- An FTIR analysis shows that saccharide enhances the H-bonded network of water by Asp

Keywords Compressibility parameters, Transfer properties, Free volume, Acoustic impedance, Ion-hydrophilic interactions, FTIR spectral analysis

*Correspondence:
Sulochana Singh
sulochanasingh@soa.ac.in

Introduction

The interactions between amino acids and saccharides in aqueous environments are of great significance due to their impact on protein stability, biological processes, and fundamental research. These interactions involve non-covalent bonds such as hydrophobic and electrostatic interactions, and hydrogen bonding, which play a crucial role in maintaining protein structure and stabilizing biological macromolecules. Study of amino acid-saccharide interactions enables the development of new materials, drugs, environmental solutions, food products, and much more, ultimately contributing to technological progress and improving quality of life. As an extension of our earlier research [1–6], we have attempted to investigate the interactions between Asp and saccharides in an aqueous media using spectroscopic and acoustic measurement. Since amino acids serve as the foundation of all living organisms, their physicochemical and thermodynamic characteristics are of great importance. These properties provide important insights that help us understand protein in aqueous medium better [7, 8]. Though there has always been a lot of interest in studies on protein stability, low molecular weight molecules (amino acids) are often used for these studies due to the challenges that arise from proteins' huge molecular weights and complicated structures. In order to understand the mechanism of molecular interactions that occur in various biochemical processes in the human body, it is crucial to examine the physicochemical characteristics of amino acids in mixed aqueous solutions [9–13]. Asp and L-arabinose/D-xylose are now taken into consideration as part of our ongoing research on the interaction of amino acids and carbohydrates having biological significance. In the central nervous system, Asp functions as an excitatory neurotransmitter. It plays a role in the nerve impulse transmission process, especially in the brain, where it aids in the communication of nerve cells. Asp plays a crucial role in the citric acid cycle, which is the primary metabolic process for producing adenosine triphosphate (ATP) from proteins, lipids, and carbohydrates. This cycle is also referred to as the Krebs cycle or TCA cycle. The presence of different chemicals like sugars, ionic salts, chaotropic agents, detergents, reducing agents, metal ions, in aqueous protein solutions is known to alter the structure of proteins [14–16]. Additives such as polyhydroxy alcohols, carbohydrates and alcohols reduce the denaturation of proteins. Carbohydrates, in particular, aid in maintaining the original shape of globular proteins. Hydrophilic and hydrophobic groups coexist in monosaccharides, making them multifunctional solutes. Although, there has already been a lot of research published in the literature [7, 8, 10–13] on molecular interactions between various biomolecules such as amino acids, carbohydrates, and enzymes, utilizing physicochemical, spectroscopic, and computational techniques, the major objectives of the present investigation is to understand and analyse how the molecular interactions are affected due to the conformational modifications of the saccharides in aqueous medium. These molecules exhibit a minimal percentage of linear form in aqueous solutions, but at equilibrium, they exist in pyranose and furanose-like structures with the $-OH$ groups in distinct orientations (axial and equatorial) [10, 12]. These carbohydrates' conformational structures control the hydration behaviour. Pentoses called L-arabinose and D-xylose are the carbohydrates, widely found in the cell walls of lignocellulosic plants and are the primary building blocks of xylans. In our earlier report we published the acoustic and spectroscopic studies of L-glutamic acid (Glu) in aqueous carbohydrates solutions [6]. In addition, we have published the volumetric and viscometric characteristics of Asp in aqueous solutions of L-arabinose/D-xylose analyzing the interactions among ionic, polar and nonpolar sites of amino acid and saccharide molecule [2]. This article represents an extension work for the acoustic properties and FTIR investigation of Asp in water and in aqueous L-arabinose/D-xylose solution (2.0 wt %, 2.5 wt %, 3.0 wt %) at T = 293.15 K to 313.15 K. This study focused on the volumetric and viscometric properties to explore the interactions between Asp and saccharides in aqueous medium across the temperature range of T = (293.15–313.15 K). The outcomes of this research provided a strong foundation for understanding such systems, still there remains a need for deeper insight into the molecular and thermodynamic aspects of these interactions using advanced methodologies. The current study shifts focus to Asp**,** another essential amino acid with distinct structural and functional properties. This study aims to extend the exploration by employing acoustic, FT-IR spectroscopy, and surface tension techniques. Our earlier investigation [6] between Glu and saccharides in aqueous medium using a combination of acoustic, FT-IR, and surface tension techniques provided valuable insights into the physicochemical behavior of Asp in the presence of saccharides, L-arabinose/D-xylose (2.0 wt %, 2.5 wt %, 3.0 wt %) in water.

Experimental

Chemicals

All chemicals were used exactly as received, without any further purification. Table 1 gives details about the chemicals that were used, including information on their purity.

Solution setup

Solutions of L-arabinose/D-xylose were prepared at three different concentrations: 2.0 wt %, 2.5 wt %, and 3.0 wt %. Deionized water was used (with a specific conductance of $(2.89-3.26)\mu Scm^{-1}$). Different molal concentrations of Asp (0.01 mol kg^{-1} to 0.05 mol kg^{-1}) were prepared using the aqueous L-arabinose/D-xylose stock solutions. Weights were measured using a digital balance with an accuracy of ±0.0001 g (Model: Citizon-Synchronics Electronics Pvt. Ltd.). Solutions were made by mass. All solutions were prepared at room temperature (T=298.15 K). The experimental pressure was maintained at (P=101 kPa). The molal uncertainty of the solutions was found to be $\pm 1 \times 10^{-3}$ mol $kg^{-1.}$

Methodology

Density and viscosity measurement

The density (ρ) of freshly prepared Asp solutions at various concentrations (0.01 mol kg^{-1} to 0.05 mol kg^{-1}) was measured using an Anton Paar DMA™ 5000 M density analyzer, which was acquired from Austria. The measurements were conducted in pure water as well as in aqueous solutions containing 2.0 wt %, 2.5 wt %, and 3.0 wt % L-arabinose or D-xylose. We already covered equipment calibration in our earlier article [16]. Prior to measuring ρ data, the density analyser was calibrated at atmospheric pressure using deionized distilled water and dry air. Distilled water and then anhydrous C_2H_5OH were used to rinse the vibrator following each measurement [17]. To make sure the device was working as it should, ρ of deionized water was first tested. The device (DMA™ 5000 M) has an integrated Peltier thermostat that helps it keep its temperature constant. The sensitivity of the device is 0.000007 g/cm^3, which is equivalent to density precision. The measured density values are reported in our earlier article [2] and are also listed in the current article. A 25 mL Ostwald viscometer was used to measure the solutions' viscosities [18]. The viscometer was calibrated at experimental temperatures with deionized water. Using a thermostatic water bath, the temperature around the viscometer was controlled within ± 0.01 K. Three recordings of the flow timings were made using a digital stopwatch with an accuracy of ± 0.01 s. To make the computation easier, the data were averaged. The viscosity measurements' standard deviation was found to be within ± 1%.

Assessment of ultrasonic velocity

Using an ultrasonic interferometer, the velocity of sound waves in a liquid medium was determined. The wavelength (λ/ms)) of sound waves in the experimental liquid medium was measured using a single frequency variable path ultrasonic interferometer (Model: F-05) from Mittal Enterprises, New Delhi, India. The apparatus is made up of ultrasonic measuring cell (10 mL capacity) with a quartz crystal base and a double-walled, premium steel frame with a chromium-coated inner surface. The quartz crystal creates ultrasonic vibrations at f= 2 MHz (a set frequency) when it comes into contact with an anodic current produced by a piezoelectric generator. The value for $\lambda/2$ is obtained from the interferometer's micrometer display. An electrostatically heated water bath was used to maintain the experimental medium's temperature at 298.15 K. The ultrasonic velocity (U/ms^{-1}) was calculated using the Eq. 1. The uncertainty of the ultrasonic velocity measurement was determined to be ± 0.2 ms^{-1}.

$$U = f \times \lambda \tag{1}$$

Surface tension calculation

The presence of functional groups $-NH_2$, $-COOH$, $-OH$ and $>C=O$ in L-arabinose/D-xylose and Asp can lead to a variety of intermolecular interactions in water, which might affect solution behaviour. Temperature and concentration are additional variables that modify these interactions. Surface tension is one such feature

Table 1 Specification of chemicals

Chemicals[a]	M[b]	CAS no.[c]	Appearance	Provenance	Mass fraction purity[d]	Purification method
Asp	0.14713	56–84-8	White crystalline powder	Loba Chemie Pvt Ltd, Mumbai, India	> 0.99	Used as received
L-arabinose	0.1501	5328-37-0	Colorless crystals as prisms or needles	Sigma-Aldrich Chemicals Pvt Ltd, Bangalore, India	> 0.99	Used as received
D-xylose	0.1501	58–86-6	Colorless monoclinic needles or prisms	Sigma-Aldrich Chemicals Pvt Ltd, Bangalore, India	> 0.99	Used as received

[a] All reagents used in the experiment were of Grade A R quality

[b] The molar mass of the chemical, (kg mol^{-1})

[c] The CAS registration number, which uniquely identifies the chemical

[d] Mass fraction according to the manufacturer's declaration

of a solution. In this investigation, surface tension (γ) is computed using the Auerbach relation (Eq. 2) [19] using experimental density (ρ) and ultrasonic velocity (U) data.

$$\gamma = 6.4 \times 10^{-10} \times \rho \times U^{3}/2 \quad (2)$$

Fourier Transform Infrared (FTIR) measurement

FTIR is commonly used to identify functional groups and chemical bonds in sample solutions. In this study, an FTIR spectrophotometer (JASCO, FTIR-4600) with computer-based software for device control and data processing was utilized to report the solutions' infrared spectra. For optimal FTIR spectra and maximum signal strength, the sample was positioned close to the Attenuated Total Reflectance (ATR) evanescent wave. ATR involves a change in a strongly internally reflected infrared beam when it interacts with the sample. The FTIR spectrophotometer operated within the range of 4000–400 cm^{-1} at standard atmospheric temperature and pressure.

Results and discussion

Ultrasonic properties

Ultrasonic properties are the key indicators of molecular interactions within solutions, revealing insights into hydrogen bonding, van der Waals forces, and ionic interactions. Changes in ultrasonic properties also highlight structural variations in solutes and solvents caused by factors like temperature or concentration. Additionally, Ultrasonic properties help deduce thermodynamic properties such as density, viscosity, and thermal behaviour, making it a valuable tool for applications in fields like material science, medicine, and biochemistry. Understanding the behavior of amino acids in mixed solvent systems by ultrasonic properties analysis, can have applications in biochemistry and food science. Using ultrasonic properties analysis to understand how amino acids behave in mixed solvent systems can be useful in food science and biology.

Sound velocity

The ultrasonic velocity or sound velocity, U of a solution, refers to the speed at which ultrasonic waves propagate through that solution. The behaviour of intra- and intermolecular interactions, complex formation, and related structural changes taking place inside the liquid solutions are all studied with great benefit by using ultrasonic speed measurements. The speed of sound for solutions of Asp + L-arabinose/D-xylose + water having varied concentrations (0.01 mol kg^{-1} to 0.05 mol kg^{-1}) was experimentally determined across different temperatures (293.15 K to 313.15 K) under constant pressure, P =101 kPa. The calculated ultrasonic velocity values are presented in Table 2. Additionally, a literature review on the ultrasonic values of Asp solutions in water was conducted. Comparisons were done between the experimental and comparable values in the literature, and there were very few cases where the concentrations of the solutions matched those of our experimental solutions [20–23]. As can be seen from the Fig. 1, the experimental data is very close to the literature data (except Ref. [20]) at almost all concentrations. The experimental ultrasonic velocity values obtained in this study, as well as those reported in one of the literature sources, are presented [20], differ from one another. However, the deviations of current results with the literature value may be due to several factors. Experimental conditions like variations in temperature, pressure, or concentration during experiments can significantly affect ultrasonic velocity. Impurities in the solute or solvent can alter molecular interactions, leading to discrepancies. Calibration issues, sensitivity of the ultrasonic equipment or measurement inaccuracies can contribute to deviations. Because the experimental results correspond well with the other papers that were highlighted. For a clear comparison, a graphical depiction is displayed. The variation in U and the resultant parameters, as influenced by solvent composition and concentration, are qualitatively examined. The observed trends are consistent with values reported in the existing literature. In a similar manner, the solvents' (aqueous L-arabinose/D-xylose) ultrasonic velocities are compared to the data from the literature and found to be consistent [24]. The ultrasonic velocity increases with the rise in Asp concentration (0.01 mol kg^{-1} to 0.05 mol kg^{-1}). The increase in the ultrasonic velocity, i.e. speed of sound in an aqueous solution can be attributed to the complex interplay of hydrogen bonding interactions: (i) the three-dimensional hydrogen bonding network in water itself, (ii) intermolecular hydrogen bonds between water and solute molecules and (iii) hydrogen bonding occurring inside the solute molecules. These interactions collectively contribute to increasing the density and elasticity of the mixture, which in turn increases the speed at which sound propagates through it [25]. The ultrasonic velocity for Asp is larger in aqueous saccharide (s) than in pure water, as Table 2 clearly shows. This suggests that when cosolute L-arabinose/D-xylose is present, more molecular interactions take place for aqueous Asp solutions. Due to the addition of cosolute the bonds break between water and Asp, Table 2 also shows that the speed of sound increases when the composition of L-arabinose/D-xylose in an aqueous medium increases. The observed variations in sound speed values can be attributed to this intricate interaction between hydrogen

Table 2 Density (ρ), ultrasonic velocity (U), viscosity (η), and compressibility parameters $\left(K_s, K_{s,\phi}\right)$ of Asp in water and aqueous L-arabinose/D-xylose at various temperatures and concentrations, and experimental pressure $P = 101$ kPa

m/(mol kg^{-1})	ρ/(Kg m^{-3})	ηx10^3/(kg m^{-1}s^{-1})	U/(m s^{-1})	$K_s \times 10^{10}$/(m^{2}N^{-1})	$K_{s,\phi} \times 10^{13}$/(m^{5}mol^{-1}N^{-1})	$K_T \times 10^{10}$ (m^{2}N^{-1})
293.15 K						
Asp in water						
0.000	998.29	1.002	1484.80			
0.009	999.03	1.010	1489.20	4.51	− 4.12	6.18
0.021	999.82	1.015	1490.80	4.50	− 2.40	6.16
0.030	1000.66	1.019	1492.40	4.49	− 1.98	6.14
0.041	1001.54	1.022	1493.20	4.48	− 1.65	6.13
0.048	1002.42	1.025	1494.40	4.47	− 1.49	6.11
Asp in L-arabinose (2.0 wt %)						
0.000	1005.61	1.043	1490.40			
0.011	1006.10	1.047	1495.20	4.44	− 3.57	6.07
0.020	1006.59	1.051	1496.80	4.43	− 2.18	6.05
0.031	1007.09	1.054	1498.40	4.42	− 1.72	6.04
0.040	1007.59	1.058	1500.00	4.41	− 1.49	6.02
0.049	1008.09	1.062	1501.60	4.39	− 1.35	6.00
Asp in L-arabinose (2.5 wt %)						
0.000	1007.12	1.051	1494.40			
0.009	1007.62	1.056	1500.80	4.41	− 3.53	6.02
0.021	1008.11	1.060	1502.40	4.39	− 2.16	6.00
0.032	1008.62	1.063	1504.00	4.38	− 1.70	5.98
0.041	1009.12	1.067	1505.60	4.37	− 1.47	5.97
0.050	1009.63	1.072	1507.20	4.36	− 1.33	5.95
Asp in L-arabinose (3.0 wt %)						
0.000	1009.70	1.075	1499.20			
0.010	1010.20	1.080	1504.40	4.37	− 3.50	5.97
0.019	1010.70	1.084	1506.00	4.36	− 2.14	5.95
0.031	1011.21	1.088	1507.60	4.35	− 1.68	5.94
0.041	1011.72	1.092	1509.20	4.34	− 1.46	5.92
0.050	1012.23	1.096	1510.80	4.33	− 1.32	5.90
Asp in D-xylose (2.0 wt %)						
0.000	1005.42	1.037	1488.40			
0.009	1005.92	1.041	1495.20	4.45	− 3.59	6.08
0.021	1006.42	1.045	1496.80	4.43	− 2.20	6.06
0.030	1006.93	1.048	1498.40	4.42	− 1.73	6.04
0.041	1007.44	1.053	1500.00	4.41	− 1.50	6.03
0.049	1007.95	1.057	1501.60	4.40	− 1.36	6.01
Asp in D-xylose (2.5 wt %)						
0.000	1006.92	1.049	1492.40			
0.011	1007.43	1.054	1500.00	4.41	− 3.56	6.03
0.020	1007.93	1.057	1501.60	4.40	− 2.17	6.01
0.029	1008.44	1.060	1503.20	4.39	− 1.71	5.99
0.041	1008.96	1.063	1504.80	4.38	− 1.49	5.98
0.051	1009.48	1.070	1506.40	4.37	− 1.35	5.96
Asp in D-xylose (3.0 wt %)						
0.000	1009.55	1.071	1497.20			
0.012	1010.06	1.076	1503.20	4.38	− 3.51	5.98
0.019	1010.57	1.079	1504.80	4.37	− 2.15	5.96

Table 2 (continued)

m/(mol kg^{-1})	ρ/(Kg m^{-3})	ηx10^3 /(kg m^{-1}s^{-1})	U/(m s^{-1})	$K_s \times 10^{10}$/(m^{2}N^{-1})	$K_{s,\phi} \times 10^{13}$/(m^{5}mol^{-1}N^{-1})	$K_T \times 10^{10}$ (m^{2}N^{-1})
0.030	1011.08	1.083	1506.40	4.36	− 1.69	5.95
0.041	1011.59	1.086	1508.00	4.35	− 1.47	5.93
0.051	1012.11	1.090	1509.60	4.34	− 1.33	5.91
298.15 K						
Asp in water						
0.000	997.13	0.889	1496.00			
0.009	997.85	0.897	1498.40	4.46	− 4.41	6.07
0.021	998.63	0.901	1499.60	4.45	− 3.29	6.05
0.030	999.47	0.904	1501.20	4.44	− 2.67	6.03
0.041	1000.35	0.907	1502.40	4.43	− 2.48	6.02
0.048	1001.21	0.910	1503.60	4.42	− 2.51	6.00
Asp in L-arabinose (2.0 wt %)						
0.000	1004.42	0.904	1496.4			
0.011	1004.91	0.908	1511.20	4.44	− 2.96	6.03
0.020	1005.40	0.911	1512.80	4.43	− 2.18	6.01
0.031	1005.89	0.915	1514.40	4.42	− 1.71	5.99
0.040	1006.38	0.918	1516.00	4.41	− 1.48	5.98
0.049	1006.88	0.921	1517.60	4.40	− 1.34	5.96
Asp in L-arabinose (2.5 wt %)						
0.000	1005.79	0.910	1500.80			
0.011	1006.28	0.914	1515.20	4.33	− 2.95	5.87
0.020	1006.77	0.918	1516.80	4.32	− 2.10	5.85
0.031	1007.27	0.921	1518.40	4.31	− 1.65	5.84
0.040	1007.77	0.925	1520.00	4.29	− 1.43	5.82
0.049	1008.27	0.927	1521.60	4.28	− 1.30	5.81
Asp in L-arabinose (3 wt %)						
0.000	1008.54	0.926	1504.80			
0.011	1009.04	0.931	1518.40	4.30	− 2.91	5.82
0.020	1009.54	0.934	1520.00	4.29	− 2.08	5.81
0.031	1010.04	0.938	1521.60	4.28	− 1.64	5.79
0.040	1010.55	0.942	1523.20	4.27	− 1.42	5.78
0.049	1011.06	0.945	1524.80	4.25	− 1.29	5.76
Asp in D-xylose (2.0 wt %)						
0.000	1004.25	0.902	1495.60			
0.011	1004.75	0.906	1509.20	4.37	− 3.22	5.93
0.020	1005.25	0.909	1510.80	4.36	− 2.12	5.91
0.031	1005.75	0.912	1512.40	4.35	− 1.67	5.90
0.040	1006.26	0.915	1514.00	4.34	− 1.44	5.88
0.049	1006.77	0.919	1515.60	4.32	− 1.31	5.86
Asp in D-xylose (2.5 wt %)						
0.000	1005.60	0.905	1500.00			
0.011	1006.10	0.910	1513.20	4.34	− 3.09	5.89
0.020	1006.60	0.912	1514.80	4.33	− 2.02	5.87
0.031	1007.11	0.914	1516.40	4.32	− 1.60	5.85
0.040	1007.62	0.917	1518.00	4.31	− 1.40	5.84
0.049	1008.14	0.922	1519.60	4.30	− 1.27	5.82
Asp in D-xylose (3.0 wt %)						
0.000	1008.38	0.926	1504.00			

Table 2 (continued)

m/(mol kg^{-1})	ρ/(Kg m^{-3})	ηx10^3 /(kg m^{-1}s^{-1})	U/(m s^{-1})	$K_s \times 10^{10}$/(m^{2}N^{-1})	$K_{s,\phi} \times 10^{13}$/(m^{5}mol^{-1}N^{-1})	$K_T \times 10^{10}$ (m^{2}N^{-1})
0.011	1008.89	0.928	1517.20	4.31	− 3.00	5.83
0.020	1009.39	0.931	1518.80	4.29	− 1.78	5.82
0.031	1009.90	0.934	1520.40	4.28	− 1.45	5.80
0.040	1010.42	0.937	1522.00	4.27	− 1.28	5.79
0.049	1010.94	0.940	1523.60	4.26	− 1.18	5.77
303.15 K						
Asp in water						
0.000	995.71	0.805	1502.80			
0.009	996.41	0.811	1507.60	4.29	− 3.80	5.96
0.021	997.16	0.815	1508.40	4.28	− 2.18	5.95
0.030	997.97	0.818	1510.00	4.27	− 1.81	5.93
0.041	998.87	0.820	1511.60	4.25	− 1.64	5.91
0.048	999.7	0.823	1512.80	4.24	− 1.48	5.90
Asp in L-arabinose (2.0 wt %)						
0.000	1002.91	0.808	1508.40			
0.011	1003.39	0.817	1514.40	4.35	− 3.79	5.90
0.020	1003.87	0.820	1515.20	4.34	− 2.05	5.89
0.031	1004.36	0.823	1516.80	4.33	− 1.62	5.87
0.040	1004.85	0.825	1519.20	4.31	− 1.52	5.85
0.049	1005.34	0.828	1520.80	4.30	− 1.37	5.83
Asp in L-arabinose (2.5 wt %)						
0.000	1004.32	0.813	1512.40			
0.011	1004.81	0.812	1519.20	4.31	− 3.76	5.85
0.020	1005.30	0.815	1520.00	4.31	− 2.03	5.84
0.031	1005.79	0.818	1521.60	4.29	− 1.61	5.83
0.040	1006.29	0.821	1524.00	4.28	− 1.51	5.80
0.049	1006.79	0.824	1525.60	4.27	− 1.36	5.79
Asp in L-arabinose (3 wt %)						
0.000	1007.25	0.829	1517.20			
0.011	1007.74	0.833	1522.80	4.28	− 3.72	5.80
0.020	1008.24	0.836	1523.60	4.27	− 2.01	5.79
0.031	1008.73	0.839	1525.20	4.26	− 1.59	5.78
0.040	1009.23	0.842	1527.60	4.25	− 1.49	5.75
0.049	1009.74	0.844	1529.20	4.24	− 1.34	5.74
Asp in D-xylose (2.0 wt %)						
0.000	1002.73	0.811	1506.40			
0.011	1003.22	0.814	1513.60	4.35	− 3.83	5.91
0.020	1003.72	0.817	1514.40	4.34	− 2.07	5.90
0.031	1004.23	0.820	1516.00	4.33	− 1.64	5.88
0.040	1004.73	0.823	1518.40	4.32	− 1.54	5.86
0.049	1005.24	0.826	1520.00	4.31	− 1.39	5.84
Asp in D-xylose (2.5 wt %)						
0.000	1004.15	0.806	1510.40			
0.011	1004.65	0.810	1518.40	4.32	− 3.79	5.86
0.020	1005.14	0.812	1519.20	4.31	− 2.04	5.85
0.031	1005.65	0.815	1520.80	4.30	− 1.62	5.83
0.040	1006.15	0.818	1523.20	4.28	− 1.52	5.81
0.049	1006.66	0.821	1524.80	4.27	− 1.37	5.79

Table 2 (continued)

m/(mol kg^{-1})	ρ/(Kg m^{-3})	ηx10^3 /(kg m^{-1}s^{-1})	U/(m s^{-1})	$K_s \times 10^{10}$/(m^{2}N^{-1})	$K_{s,\phi} \times 10^{13}$/(m^{5}mol^{-1}N^{-1})	$K_T \times 10^{10}$ (m^{2}N^{-1})
Asp in D-xylose (3.0 wt %)						
0.000	1007.09	0.810	1515.20			
0.011	1007.59	0.815	1521.60	4.29	− 3.75	5.81
0.020	1008.09	0.817	1522.40	4.28	− 2.03	5.80
0.031	1008.60	0.820	1524.00	4.27	− 1.60	5.79
0.040	1009.11	0.823	1526.40	4.25	− 1.50	5.76
0.049	1009.62	0.826	1528.00	4.24	− 1.35	5.75
308.15 K						
Asp in water						
0.000	994.08	0.723	1508.00			
0.009	994.76	0.728	1519.50	4.35	− 6.00	5.84
0.021	995.49	0.732	1520.30	4.35	− 3.26	5.83
0.030	996.30	0.734	1520.90	4.34	− 2.33	5.82
0.041	997.17	0.736	1522.50	4.33	− 2.03	5.80
0.048	998.03	0.738	1523.70	4.32	− 1.79	5.78
Asp in L-arabinose (2.0 wt %)						
0.000	1001.05	0.729	1518.30			
0.011	1001.53	0.732	1524.30	4.30	− 3.74	5.82
0.020	1002.00	0.735	1525.10	4.29	− 2.01	5.81
0.031	1002.49	0.737	1526.70	4.28	− 1.59	5.80
0.040	1002.98	0.739	1529.10	4.26	− 1.49	5.78
0.049	1003.47	0.742	1530.70	4.25	− 1.34	5.76
Asp in L-arabinose (2.5 wt %)						
0.000	1002.31	0.732	1522.30			
0.011	1002.79	0.735	1529.10	4.26	− 3.70	5.79
0.020	1003.28	0.738	1529.90	4.26	− 2.00	5.78
0.031	1003.76	0.741	1531.50	4.25	− 1.58	5.77
0.040	1004.26	0.742	1533.90	4.23	− 1.48	5.74
0.049	1004.75	0.745	1535.50	4.22	− 1.33	5.73
Asp in L-arabinose (3 wt %)						
0.000	1004.44	0.737	1527.10			
0.011	1004.93	0.741	1532.70	4.24	− 3.67	5.75
0.020	1005.42	0.744	1533.50	4.23	− 1.98	5.74
0.031	1005.91	0.747	1535.10	4.22	− 1.56	5.72
0.040	1006.41	0.749	1537.50	4.20	− 1.47	5.70
0.049	1006.91	0.751	1539.10	4.19	− 1.32	5.68
Asp in D-xylose (2.0 wt %)						
0.000	1000.87	0.727	1516.30			
0.011	1001.36	0.730	1523.50	4.30	− 3.78	5.84
0.020	1001.86	0.732	1524.30	4.30	− 2.04	5.83
0.031	1002.36	0.734	1525.90	4.28	− 1.62	5.82
0.040	1002.87	0.737	1528.30	4.27	− 1.52	5.80
0.049	1003.38	0.740	1529.90	4.26	− 1.37	5.78
Asp in D-xylose (2.5 wt %)						
0.000	1002.42	0.730	1520.30			
0.011	1002.91	0.733	1528.30	4.27	− 3.72	5.80
0.020	1003.43	0.735	1529.10	4.26	− 2.01	5.79
0.031	1003.96	0.738	1530.70	4.25	− 1.59	5.77

Table 2 (continued)

$m/(\text{mol kg}^{-1})$	$\rho/(\text{Kg m}^{-3})$	$\eta x10^3/(\text{kg m}^{-1}\text{s}^{-1})$	$U/(\text{m s}^{-1})$	$K_s \times 10^{10}/(\text{m}^2\text{N}^{-1})$	$K_{s,\phi} \times 10^{13}/(\text{m}^5\text{mol}^{-1}\text{N}^{-1})$	$K_T \times 10^{10}$ $(\text{m}^2\text{N}^{-1})$
0.040	1004.43	0.741	1533.10	4.24	− 1.49	5.75
0.049	1004.97	0.743	1534.70	4.23	− 1.34	5.73
Asp in D-xylose (3.0 wt %)						
0.000	1004.29	0.732	1525.10			
0.011	1004.79	0.736	1531.50	4.24	− 3.69	5.76
0.020	1005.28	0.738	1532.30	4.24	− 1.99	5.75
0.031	1005.78	0.740	1533.90	4.23	− 1.58	5.73
0.040	1006.29	0.743	1536.30	4.21	− 1.48	5.71
0.049	1006.80	0.746	1537.90	4.20	− 1.33	5.69
313.15 K						
Asp in water						
0.000	992.25	0.652	1515.20			
0.009	992.91	0.657	1526.50	4.32	− 5.21	5.76
0.021	993.62	0.660	1527.30	4.31	− 4.85	5.75
0.030	994.43	0.661	1527.90	4.31	− 3.39	5.74
0.041	995.28	0.664	1529.50	4.29	− 2.82	5.72
0.048	996.1	0.665	1530.70	4.28	− 2.42	5.70
Asp in L-arabinose (2.0 wt %)						
0.000	999.24	0.662	1528.29			
0.011	999.71	0.665	1534.30	4.25	− 3.67	5.78
0.020	1000.18	0.667	1535.10	4.24	− 1.97	5.77
0.031	1000.66	0.670	1536.70	4.23	− 1.56	5.75
0.040	1001.14	0.671	1539.10	4.22	− 1.46	5.73
0.049	1001.63	0.674	1540.70	4.21	− 1.32	5.71
Asp in L-arabinose (2.5 wt %)						
0.000	1000.91	0.667	1532.29			
0.011	1001.39	0.670	1539.10	4.22	− 3.64	5.73
0.020	1001.87	0.673	1539.90	4.21	− 1.96	5.72
0.031	1002.36	0.675	1541.50	4.20	− 1.55	5.70
0.040	1002.84	0.677	1543.90	4.18	− 1.45	5.68
0.049	1003.34	0.679	1545.50	4.17	− 1.31	5.66
Asp in L-arabinose (3 wt %)						
0.000	1003.26	0.671	1537.09			
0.011	1003.74	0.675	1542.70	4.19	− 3.60	5.68
0.020	1004.23	0.678	1543.50	4.18	− 1.94	5.67
0.031	1004.72	0.680	1545.10	4.17	− 1.53	5.66
0.040	1005.21	0.682	1547.50	4.15	− 1.44	5.64
0.049	1005.71	0.684	1549.10	4.14	− 1.29	5.62
Asp in D-xylose (2.0 wt %)						
0.000	999.05	0.661	1526.29			
0.011	999.53	0.663	1533.50	4.25	− 3.72	5.78
0.020	1000.03	0.665	1534.30	4.25	− 2.01	5.77
0.031	1000.53	0.667	1535.90	4.24	− 1.59	5.76
0.040	1001.04	0.669	1538.30	4.22	− 1.49	5.74
0.049	1001.55	0.672	1539.90	4.21	− 1.34	5.72
Asp in D-xylose (2.5 wt %)						
0.000	1000.70	0.664	1530.29			
0.011	1001.19	0.668	1538.30	4.22	− 3.66	5.73

Table 2 (continued)

$m/(\text{mol kg}^{-1})$	$\rho/(\text{Kg m}^{-3})$	$\eta x10^3/(\text{kg m}^{-1}\text{s}^{-1})$	$U/(\text{m s}^{-1})$	$K_s \times 10^{10}/(\text{m}^2\text{N}^{-1})$	$K_{s,\phi} \times 10^{13}/(\text{m}^5\text{mol}^{-1}\text{N}^{-1})$	$K_T \times 10^{10}$ $(\text{m}^2\text{N}^{-1})$
0.020	1001.68	0.670	1539.10	4.21	− 1.98	5.72
0.031	1002.18	0.672	1540.70	4.20	− 1.56	5.71
0.040	1002.68	0.675	1543.10	4.19	− 1.47	5.69
0.049	1003.18	0.677	1544.70	4.18	− 1.32	5.67
Asp in D-xylose (3.0 wt %)						
0.000	1003.10	0.667	1535.09			
0.011	1003.59	0.671	1541.50	4.19	− 3.62	5.69
0.020	1004.08	0.672	1542.30	4.19	− 1.95	5.68
0.031	1004.58	0.675	1543.90	4.18	− 1.55	5.67
0.040	1005.08	0.677	1546.30	4.16	− 1.45	5.65
0.049	1005.58	0.680	1547.90	4.15	− 1.30	5.63

Standard uncertainties:$u(m_A) = 1 \times 10^{-3}$ mol kg^{-1} (confidence level of 0.68), u (wt %) = ± 0.05 wt %, u (*T*) = 0.01 K, u(p) = 1.0 kPa. The combined uncertainties (with a 0.95 level of confidence) for $U(\rho) = 0.45$ kg m^{-3},$U(K_s) = 0.005 \times 10^{-10}$Pa^{-1}, $U(K_{s,\phi}) = 0.081 \times 10^{-14}$m^{3}mol^{-1}Pa^{-1}

bond formation and rupture. Comparing the U values of Asp + L-arabinose/D-xylose + water solutions with that of Glu + L-arabinose/D-xylose + water solutions [6] it is observed that U values are less in the former system than that of the later. The difference in U values between Asp and Glu in the same solvent can be attributed to their molecular structures and interactions with the solvent. Asp has a shorter side chain compared to Glu, which results in different solvation behaviors. The shorter side chain of Asp leads to a more compact structure, allowing for stronger interactions with the solvent molecules. This increased interaction with the solvent molecules results in higher compressibility and lower ultrasonic velocity. On the other hand, Glu has a longer side chain, which makes its structure more extended. This extended structure leads to weaker interactions with the solvent molecules, resulting in lower compressibility and higher ultrasonic velocity. Correspondingly, the other properties of the Asp solutions can be compared with the properties of Glu solutions, focusing on their molecular structures and solvent interactions.

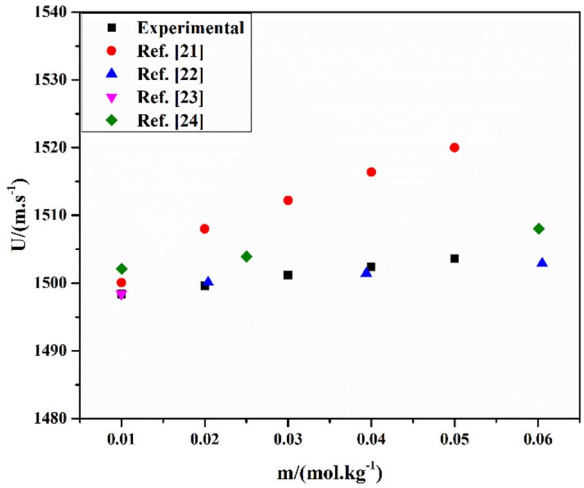

Fig. 1 A comparison of experimental and literature ultrasonic velocity values (*U*) of aqueous Asp at 298.15 K

Additionally, Table 2 demonstrates that aqueous L-arabinose solutions have greater ultrasonic velocity values of Asp than aqueous D-xylose solutions. A similar observation was also obtained for Glu in aqueous L-arabinose/D-xylose [6]. These features result from the stereochemical differences between xylose and arabinose, even though both are pentoses. In water, the main conformation of L-arabinose is 1e2e3e4a, while that of D-xylose is 1e2e3e4e [26]. Due to this, D-xylose better comply with water than L-arabinose. Compared to the latter, the former has stronger hydrogen bonds with water. Hence, greater molecular association on the hydration of Asp as well as the associative connection between ions ($-COO^-$, $-NH_3^+$) of Asp and hydrophilic regions of L-arabinose in water are indicated by a rising trend in ultrasonic velocity readings than in D-xylose. The change of U with respect to Asp molality in L-arabinose/D-xylose + water at 298.15 K is shown graphically in Fig. 2. A similar trend is followed at all other temperatures.

Compressibility parameters

Isentropic compressibility (K_s) and isothermal compressibility (K_T)

The term compressibility, often known as the coefficient of compressibility, in thermodynamics describes how a system's volume changes proportionately when pressure changes. Isentropic compressibility is the thermodynamic property that characterizes a substance's relative

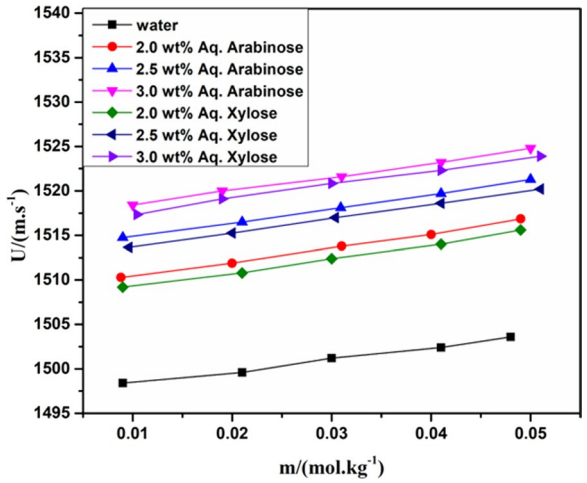

Fig. 2 Ultrasonic velocity, *U* of Asp in aqueous L-arabinose and D-xylose at 298.15 K

change in volume in response to a change in pressure while maintaining a constant entropy. Isothermal compressibility, on the other hand, refers to the relative change in volume of a material in reaction to a change in pressure while keeping the temperature constant. These two parameters have the following mathematical expressions (Eqs. 3 & 4) [27]:

$$K_S = -\frac{1}{V}\left(\frac{\partial V}{\partial P}\right)_S \tag{3}$$

$$K_T = -\frac{1}{V}\left(\frac{\partial V}{\partial P}\right)_T \tag{4}$$

where, *T, P, V* denotes the temperature, pressure, volume, and *s* denotes that the process is isentropic (adiabatic and reversible).

K_s can also be calculated using the Newton–Laplace Eq. (5) [28].

$$K_s = 1/\left(\rho U^2\right) \tag{5}$$

where U and ρ represents the speed of sound and density of the medium. The values for isentropic compressibility K_s are listed in Table 2. The uncertainty in K_s was determined to be $\pm 0.004 \times 10^{-10}$ Pa^{-1} using Eq. (6).

$$\partial K_s = K_s \times \left[(2\partial u/u)^2 + (\partial\rho/\rho^2\right]^{1/2} \tag{6}$$

It is assumed that in electrolyte solutions the isentropic compressibility is equal to the sum of the solute's and solvent's intrinsic isentropic compressibilities, i.e. $K_{s(solute\ intrinsic)}$ and $K_{s(solvent\ intrinsic)}$, respectively. The term "intrinsic compressibility" describes a solvent's innate capacity to compress under pressure without being considerably impacted by outside variables, such as dissolved solutes, whereas the molecular structure, conformational flexibility, and intermolecular interactions of a solute can all have an impact on its intrinsic compressibility. Solvent intrinsic compressibility originates from the compression of water's three-dimensional network structure. In contrast, solute intrinsic compressibility arises from the compression of ions' hydration shells. Since the hydration shells exhibit minimal compressibility, the solvent intrinsic compressibility is considered the primary contributing factor [29].

More molecules of solvent get involved in the development of solvation shells as the solute concentration rises, where they are subjected to severe electrostriction provided by the trapped ions. The solvation shells are, therefore, compressed and their capacity to compress further is diminished. This effect is demonstrated by the pattern of K_s falling as Asp and saccharide(s) content rise. A graphical presentation is given (Fig. 3) for the variation of K_s with concentration of Asp and solvent (aqueous L-arabinose/D-xylose) compositions of 2.0 wt %, 2.5 wt % and 3.0 wt % at 298.15 K. Figure 3 illustrates that as temperatures increase, water molecule's 3D structure is disrupted, leading to greater hydration of Asp molecules. This observation aligns with the results of volumetric measurements [2]. Same pattern of K_s for Asp in all the compositions of saccharides is also obtained at other temperatures.

The linear relation between the isentropic compressibility and solute's molality is expressed by Eq. (7).

$$K_s = K_s^0 + S_K\sqrt{m} \tag{7}$$

The K_s vs. $\sqrt{m}$ figure can be extended to the Y-axis to determine the limiting or partial isentropic compressibility, K_s^0. The isentropic compressibility at infinite dilution is represented by these values. The slope of the line, which represents ion pair interactions, indicates another crucial parameter, S_K. The interactions between individual solute ions are minimal under infinite dilution circumstances because a sizable volume of solvent effectively separates the solute particles. The solvent molecules and the Asp ions interact most frequently in aqueous Asp solutions.

It is impossible to ignore connections among saccharides' polar moieties and the zwitterionic ions ($-COO^-$, $-NH_3^+$) and the side chain carboxylate ion ($-COO^-$) of Asp, even at infinite dilution with saccharides in solution. The saccharide(s) concentration causes ion-ion interactions to rise

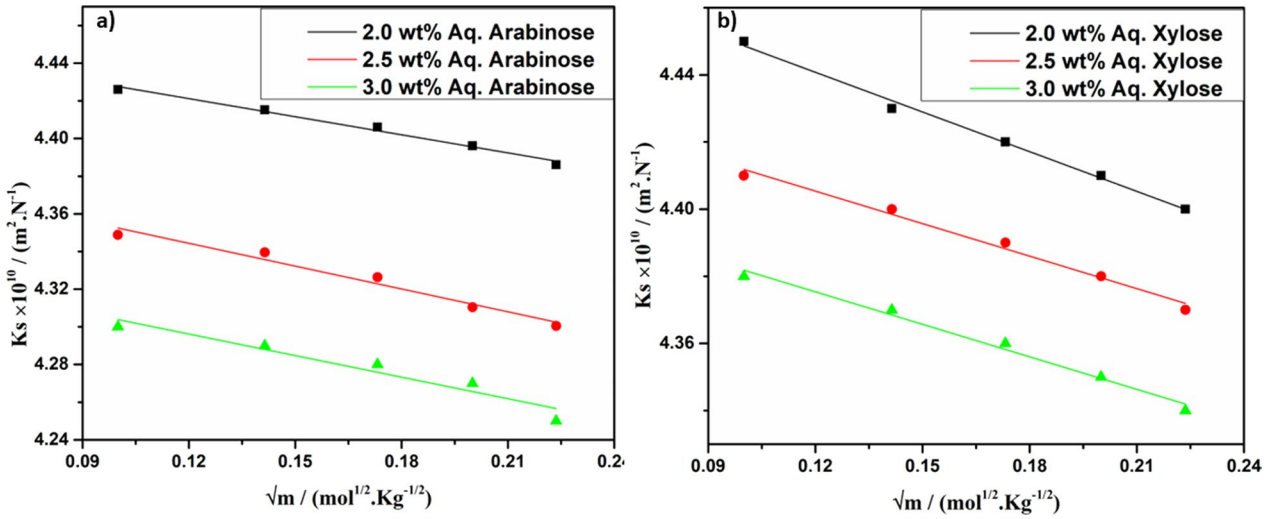

Fig. 3 Isentropic compressibility, K_s vs square root of molality, $\sqrt{m}$ for Asp in aqueous **a** 2.0, 2.5, 3.0 wt % arabinose, **b** 2.0, 2.5, 3.0 wt % xylose at 298.15 K

while ion–solvent interactions progressively decrease. Table 3 displays the values for K_s^0 and S_K. The stronger ion–solvent interactions than ion–ion interactions are demonstrated by the greater and positive values of K_s^0 in comparison to the lower and negative values of S_K for all of the solutions studied.

Compressibility under isothermal conditions K_T is a key parameter that provides insights into the physical, mechanical, and thermodynamic properties of substances across a wide range of disciplines, from material science to geophysics to biology. In addition, studying isothermal compressibility K_T is valuable for unravelling the intricate interplay between different segments present in solutions, particularly in systems with diverse interactions, such as those involving ionic, hydrophilic, and hydrophobic components. The following Eq. (8) is used to calculate K_T [30].

$$K_T = \left(171/(T^{4/9}\rho^{4/3}U^2\right) \tag{8}$$

Table 2 documents isentropic compressibility values, K_s, and isothermal compressibility values, K_T. The table illustrates how K_T varies with Asp and L-arabinose/D-xylose concentrations, which often follow the similar pattern as K_s. Because of the strong ion–solvent interactions and the electrostriction of the hydration shells, both of the compressibility parameters encourage the loss of compressibility.

Apparent molar isentropic compressibility $\left(K_{s,\phi}\right)$

The apparent molar isentropic compressibility, denoted as $K_{s,\phi}$, is a thermodynamic property that describes the volume change (compressibility) of a solution with each mole of solute added while entropy is constant. ϕ usually refers to the species or solute component in the solution. It is a measurement of how the addition of solute molecules alters the solution's compressibility while taking solvent–solvent and solute–solvent interactions into consideration. When solute ions are dissolved in an aqueous solution, water molecules play a part in the process. By forming solvation layers surrounding the ions, water molecules ensnare the ions of solute. The water molecules that are subjected to structural deformation inside the ions'electrostatic field are strongly electrostrictively pulled by these ions. Near the ions, the water molecules are almost noncompressible because they are closely packed. Conversely, bulk water molecules, or those outside the ions'electrostatic field, are not constrained by electrostriction and can compress. Apparent molar isentropic compressibility refers to the relative compressibility of water molecules in these two distinct settings [31]. $K_{s,\phi}$ values for Asp in aqueous saccharide(s) solutions at T = 293.15 K–313.15 K are calculated using the relation given below (Eq. 9) [32], and the values are listed in Table 2.

$$K_{s,\phi} = \left(K_s\rho_0 - K_s^0\rho\right)/m\rho\rho_0 + MK_s/\rho \tag{9}$$

Table 3 Values of $\left(K_s^0\right)$, $\left(S_K\right)\left(K_{s,\phi}^0\right)$, $\left(S_{K,\phi}\right)$ and $\left(K_{s,\phi,tr}^0\right)$ for Asp in water, aqueous L-arabinose/D-xylose at 293.15 K, 298.15 K, 303.15, 308.15 K, 313.15 K and experimental pressure P = 101 kPa

Composition of solution	$K_s^0 \times 10^{10}$/(m^2N^{-1})	$S_K \times 10^{11}$/($m^2N^{-1}mol^{-1/2}kg^{1/2}$)	$K_{s,\phi}^0 \times 10^{13}$/($m^5mol^{-1}N^{-1}$)	$S_{k,\phi} \times 10^{12}$/($m^5N^{-1}mol^{-3/2}kg^{1/2}$)	$\Delta_{tr}K_{s,\phi}^0 \times 10^{13}$/($m^5mol^{-1}N^{-1}$)
293.15 K					
Water	5.75 ± 0.01	− 3.74 ± 0.18	−5.75 ± 0.84	2.04 ± 0.48	
Aq L-arabinose					
2.0 wt %	4.48 ± 0.01	− 3.77 ± 0.21	− 4.98 ± 0.93	1.74 ± 0.22	0.77
2.5 wt %	4.44 ± 0.01	− 3.71 ± 0.13	− 4.93 ± 0.48	1.72 ± 0.53	0.81
3.0 wt %	4.42 ± 0.01	− 3.68 ± 0.05	− 4.88 ± 0.75	1.71 ± 0.57	0.87
Aq D-xylose					
2.0 wt %	4.47 ± 0.01	− 3.74 ± 0.21	− 5.02 ± 0.72	1.75 ± 0.53	0.73
2.5 wt %	4.44 ± 0.03	− 3.70 ± 0.18	− 4.97 ± 0.72	1.74 ± 0.28	0.78
3.0 wt %	4.41 ± 0.01	− 3.66 ± 0.76	− 4.91 ± 0.76	1.71 ± 0.44	0.84
298.15 K					
Water	4.50 ± 0.01	− 3.73 ± 0.36	− 5.64 ± 0.83	1.87 ± 0.48	
Aq L-arabinose					
2.0 wt %	4.48 ± 0.01	− 3.74 ± 0.03	− 4.84 ± 0.07	1.47 ± 0.04	0.80
2.5 wt %	4.36 ± 0.01	− 3.61 ± 0.68	− 4.80 ± 1.11	1.46 ± 0.60	0.84
3.0 wt %	4.33 ± 0.01	− 3.59 ± 0.10	− 4.74 ± 0.59	1.45 ± 0.39	0.90
Aq D-xylose					
2.0 wt %	4.40 ± 0.01	− 3.67 ± 0.21	− 5.15 ± 0.21	1.67 ± 0.18	0.49
2.5 wt %	4.37 ± 0.01	− 3.64 ± 0.53	− 4.94 ± 0.83	1.48 ± 0.41	0.69
3.0 wt %	4.34 ± 0.01	− 3.61 ± 0.51	− 4.87 ± 0.33	1.50 ± 0.48	0.77
303.15 K					
Water	4.45 ± 0.01	− 3.70 ± 0.36	− 5.45 ± 0.83	1.77 ± 0.48	
Aq L-arabinose					
2.0 wt %	4.38 ± 0.01	− 3.72 ± 0.03	− 5.18 ± 0.07	1.85 ± 0.04	0.27
2.5 wt %	4.35 ± 0.01	− 3.69 ± 0.68	− 5.13 ± 1.11	1.83 ± 0.60	0.32
3.0 wt %	4.32 ± 0.01	− 3.66 ± 0.10	− 5.07 ± 0.59	1.81 ± 0.39	0.38
Aq D-xylose					
2.0 wt %	4.39 ± 0.01	− 3.75 ± 0.21	− 5.22 ± 0.21	1.86 ± 0.18	0.22
2.5 wt %	4.35 ± 0.01	− 3.70 ± 0.53	− 5.16 ± 0.83	1.84 ± 0.41	0.29
3.0 wt %	4.32 ± 0.01	− 3.68 ± 0.51	− 5.11 ± 0.33	1.82 ± 0.48	0.34
308.15 K					
Water	4.41 ± 0.01	− 3.70 ± 0.36	− 8.61 ± 0.83	3.29 ± 0.48	
Aq L-arabinose					
2.0 wt %	4.34 ± 0.01	− 3.65 ± 0.03	− 5.10 ± 0.07	1.82 ± 0.04	3.51
2.5 wt %	4.30 ± 0.01	− 3.62 ± 0.68	− 5.04 ± 1.11	1.80 ± 0.60	3.57
3.0 wt %	4.27 ± 0.01	− 3.60 ± 0.10	− 5.00 ± 0.59	1.79 ± 0.39	3.58
Aq D-xylose					
2.0 wt %	4.34 ± 0.01	− 3.69 ± 0.21	− 5.15 ± 0.21	1.84 ± 0.18	3.46
2.5 wt %	4.31 ± 0.01	− 3.64 ± 0.53	− 5.07 ± 0.83	1.81 ± 0.41	3.54
3.0 wt %	4.28 ± 0.01	− 3.61 ± 0.51	− 5.04 ± 0.33	1.80 ± 0.48	3.57
313.15 K					
Water	4.41 ± 0.01	− 3.01 ± 0.36	− 13.47 ± 0.83	5.33 ± 0.48	
Aq L-arabinose					
2.0 wt %	4.28 ± 0.01	− 3.59 ± 0.03	− 5.01 ± 0.07	1.79 ± 0.04	8.46
2.5 wt %	4.25 ± 0.01	− 3.56 ± 0.68	− 4.96 ± 1.11	1.76 ± 0.60	8.51
3.0 wt %	4.22 ± 0.01	− 3.53 ± 0.10	− 4.91 ± 0.59	1.78 ± 0.39	8.56
Aq D-xylose					
2.0 wt %	4.29 ± 0.01	− 3.63 ± 0.21	− 5.07 ± 0.21	1.81 ± 0.18	8.40
2.5 wt %	4.26 ± 0.01	− 3.58 ± 0.53	− 5.00 ± 0.83	1.79 ± 0.41	8.47
3.0 wt %	4.23 ± 0.01	− 3.55 ± 0.51	− 4.91 ± 0.33	1.76 ± 0.48	8.56

With a confidence level of 0.68, the standard uncertainties are u(T) = 0.01 K and u(p) = 1.0 kPa. The standard uncertainty for the solvent composition (clean water + L-arabinose/D-xylose) is u(wt %) = ± 0.05 wt %

where M and m stand for the solute's molecular mass and molality, while ρ and ρ_0 for the densities of the solute and solvent. Using the following Eq. (10) $\partial K_{s,\phi}$ was determined to be $0.082\times10^{-14}\mathrm{m^3mol^{-1}Pa^{-1}}$ at a lower molality range [33].

$$\begin{aligned}&\partial K_{s,\phi}\\&=\left\{\left[\left(MK_s/\rho\right)-K_{s,\phi}\right)(\partial m/m)\right]^2+\left[\left(K_{s,\phi}+K_s^0/m\rho_0\right)(\partial\rho/\rho)\right]^2\\&+\left[K_{s,\phi}+K_s^0/m\rho_0\right)(\partial K_s/K_s)\right]^2\Big\}^{1/2}\end{aligned}\tag{10}$$

For a given concentration of saccharide(s), the negative $K_{s,\phi}$ value diminishes as the molality of Asp increases. However, this negativity for $K_{s,\phi}$ value of Asp in pure water increases with temperature, whereas it diminishes when L-arabinose/D-xylose is present. It can be noticed that the values of $K_{s,\phi}$ for Asp is less than of Glu in aqueous L-arabinose/D-xylose [6]. The reason may be, Asp with its shorter side chain, tends to form stronger and more compact hydration shells, leading to lower compressibility. On the other hand, Glu, with its longer side chain, may have a more extended hydration structure, resulting in higher compressibility.

The size and shape of the zwitterion, the kind of solvent, and the temperature and pressure can all affect the intermolecular free space surrounding organic anions. In some cases, the arrangement of solvent molecules around the organic anion may result in relatively large spaces between them, allowing for the accommodation of additional solvent molecules. This phenomenon is particularly relevant in solution chemistry and has implications for various properties and behaviours of solutions containing organic anions [34]. Throughout the whole concentration range of Asp and L-arabinose/D-xylose, negative values of $K_{s,\phi}$ suggest solvent penetration into the intra-ionic free spaces of organic molecules. Another potential reason for the negative value of $K_{s,\phi}$ is that water molecules in the hydration shells are less compressible than those in the bulk. If we compare the $K_{s,\phi}$ values of Asp in aqueous L-arabinose and aqueous D-xylose, the negative values are higher in L-arabinose than D-xylose, i.e. the compressibility is higher in aqueous D-xylose medium. As discussed, D-xylose can better fit into the water molecules than L-arabinose, which leads to greater compressibility of the water molecules in the hydration shells compared to those in the bulk. As the concentration of Asp increases, more hydration shells are formed, leading to the loss of a greater number of water molecules from the bulk. The compressibility of the bulk drops as a result of water molecules being lost, and the gap between the compressibility of water near the solute and in the bulk narrows. Table 2 shows the variation of $K_{s,\phi}$ with Asp concentration. The properties like homochirality, stereoselectivity, and coordinating abilities, and presence of hydrophilic hydroxyl (–OH) groups in sacharides contribute to their significant role in various biochemical processes and their wide range of applications in different fields. That's why saccharides are considered a fundamental family of chemicals. The solubility of saccharides in polar solvents like water is enhanced by their hydrophilic groups, such as hydroxyl ($-OH$), carbonyl ($>C=O$), and amino ($-NH_2$) groups. When L-arabinose or D-xylose (types of saccharides) interact with water, their polar sites attract water molecules and become hydrated, forming hydration shells around them. As a result, these water molecules are no longer available to hydrate the Asp (aspartic acid) molecules. Consequently, the primary hydration shells that initially surrounded the Asp molecules lose some of their water molecules, leading to a reduction in their hydration. In essence, the hydration of L-arabinose or D-xylose causes a dehydration effect on the Asp molecules. This results in less negative $K_{s,\phi}$ values due to the increased compressibility and reduced electrostriction of water molecules in the outer solvation shells [36]. When L-arabinose or D-xylose interact with Asp, they form ion pairs with the polar groups of Asp, such as the carboxyl ($-COOH$) and amino ($-NH_2$) groups, as well as with the zwitterionic centers ($-COO^-$ and NH_3^+). This pairing means that the ions from Asp are more attracted to the saccharides rather than to water molecules. Because of this, the electrostatic interactions between Asp ions and water molecules are reduced. As a result, water molecules become more loosely packed, increasing their compressibility. Essentially, the presence of saccharides changes the way water molecules interact with each other and with Asp, making the water molecules more flexible and easier to compress.

Equation (11) is used to derive the limiting apparent molar isentropic compression,

$$K_{s,\phi}=K_{s,\phi}^0+S_{k,\phi}\sqrt{m}\tag{11}$$

The intercept of the above linear equation, called limiting apparent molar isentropic compression yields $K_{s,\phi}^0$ and the slope, called experimental slope for isentropic compression, yields $S_{k,\phi}$. Table 3 shows the values of $K_{s,\phi}^0$ and $S_{k,\phi}$ along with the standard errors. Ion-hydrophilic interactions between the solute ions and the solvent are shown by the magnitude of $K_{s,\phi}^0$, whereas ion-ion, ion-hydrophilic, and hydrophilic –hydrophilic interactions between the solute and cosolute ions and polar groups are indicated by $S_{k,\phi}$. The hydrophobic-hydrophobic interactions between (hydrophobic) carbon skeleton of L-arabinose/D-xylose's and Asp's could be the cause of $K_{s,\phi}^0$ values that are negative. It is

noteworthy that all values of $K_{s,\phi}$ are negative, and that the negativity seems to diminish as the temperature and the composition of the co-solute, L-arabinose/D-xylose, increase. Water molecules that are liberated from the bulk due to a reduction in electrostriction demonstrate the existence of strong, attractive interactions between Asp and water. In this case, the behaviour of $K^0_{s,\phi}$ values in the presence of L-arabinose/D-xylose can be explained using the Kirkwood model [35].

This model states that because electrostriction water has a more compact structure than bulk water, it is highly compressible. Therefore, when the contacts between Asp and saccharides increase, the electrostriction connections between water molecules and Asp decrease. In doing so, the solute's compressibility is further enhanced by driving electrostriction water back into the bulk through the solvation layer [36].

Partial molar isentropic compression of transfer $\left(K^0_{s,\phi,tr}\right)$

The transfer parameter of the limiting apparent molar isentropic compressibility provides insight into how the compressibility of a solution changes as solute molecules are added. Positive values indicate that the compressibility increases upon adding solute, while negative values indicate a decrease in compressibility. The values of partial molar isentropic compression of transfer, $K^0_{s,\phi,tr}$ for the Asp solution can be obtained using the relation (Eq. 12).

$$K^0_{s,\phi,tr(\text{aqueous saccharide}\rightarrow\text{water})} = K^0_{s,\phi}(\text{in aqueous saccharide}) - K^0_{s,\phi}(\text{in water}) \quad (12)$$

The values of $K^0_{s,\phi,tr}$ for Asp at every composition of supplied saccharides are positive and are indexed in Table 3. Based on the co-sphere overlap model of ternary mixtures, the solute and co-solute species in water may interact in different ways. [39, 40]. Ion-ion interactions are formed by ions such as zwitterionic ($-COO^-$ and $-NH_3^+$), $-COO^-$ of Asp and ions of L-arabinose/D-xylose in water (figure S1, supplementary material). The polar $-OH$ and $-NH_2$ groups of Asp, along with the above mentioned ions, produce hydrophilic-hydrophilic and ion-hydrophilic interactions. Ions create ion-hydrophobic and hydrophilic-hydrophobic interactions with polar groups and hydrocarbon segments of Asp, L-arabinose, and D-xylose. L-arabinose/D-xylose and Asp's alkyl backbones interact hydrophobically with one another. A study on the enthalpies of mixing aqueous solutions of glycine, L-alanine, and L-serine with aqueous solutions of fructose and sorbose, as well as the corresponding enthalpies of dilution, revealed that different $-OH$ groups of the same saccharide molecule can interact with the zwitterionic and $-OH$ groups of the L-serine molecule. In this case, the hydrophobic contacts are strengthened and the nonpolar groups of L-serine and saccharide get closer [37].

The following types of interactions can be emphasized while extrapolating the current interactions. The following interactions are listed in order of preference: Groups that are (a) nonpolar and nonpolar, (b) polar and nonpolar, (c) polar and polar, and (d) polar and ionic. $K^0_{s,\phi,tr}$ values would be positive for interactions of the forms (a) and (b), whereas $K^0_{s,\phi,tr}$ values would be negative for interactions of the other types, based on these concepts. $K^0_{s,\phi,tr}$ results indexed in Table 3 show that the (a) and (b) types of interactions between the polar groups of saccharides and the ions of Asp are prevalent in this scenario. It can also be inferred that as saccharide composition increases, $K^0_{s,\phi,tr}$ values for Asp increase as well and with increasing temperature at all concentrations of supplied saccharides $K^0_{s,\phi,tr}$ values drop. The structure forming tendency of ions is indicated by the preponderance of connections between the zwitterionic centre of Asp and polar parts of L-arabinose and D-xylose, as indicated by the positive values of $K^0_{s,\phi,tr}$. As the saccharide concentration increases, the zwitterionic centre of Asp interacts with saccharides more. As the concentration of saccharide increases, electrostriction decreases, and the propensity to form ions in structures increases. Because of this, the compressibility of electrostricted water is much less than that of bulk water, and it gets much less as the saccharide composition increases. This implies that a large number of solvent molecules have bonded to a large number of solute molecules, boosting the ions' interactions with each other [38]. Overall, the study demonstrates that the interactions between the zwitterion of Asp and polar sites of saccharide (s) cause the positive values of $K^0_{s,\phi,tr}$ to indicate the structure-making behaviour of Asp in aqueous saccharide (s) [39]. However, a study on Asp's interactions with D-glucose, D-galactose, and D-fructose using densimetry, calorimetry of dissolution, and isothermal titration calorimetry reveals Asp as a structure breaker [40].

In this study, Asp functions as a structure maker, contributing to the formation and stabilization of specific structures within the solution. Its interactions with other molecules, such as saccharides, help maintain the organization and integrity of the system being studied. The report in our recent publication [3], i.e. the negative values of the temperature derivative of the B-coefficient $\partial B_J/\partial T$, and the positive values of the Hepler's constant $\left(\partial^2 V^0_{\varnothing}/\partial T^2\right)_p$ and free energy of activation ($\Delta\mu_1^{0\#}$ *and* $\Delta\mu_2^{0,\#}$) supports this.

Interaction co-efficients

The Eq. 13 shown below allowed for the calculation of the pair and triplet interaction coefficient of isentropic compression.

$$K^0_{s,\phi,tr} = 2K_{AB}m_B + 3K_{ABB}m_B^2 + \cdots \quad (13)$$

Asp is represented by A, saccharide (s) by B, and m_B represents the molal concentration of saccharide (s).

K_{AB} is the pair interaction co-efficient and K_{ABB} is the triplet interaction co-efficient of isentropic compression. To calculate and index the pair and triplet coefficients in table S1 (supplementary material), McMillan–Mayer theory was applied [41]. This theory fits the partial molar property values for $K^0_{s,\phi,tr}$ to find the coefficients, K_{AB} and K_{ABB}. The interactions between molecules in triplets and pairs are examined using the McMillan–Mayer theory. The pair interaction coefficient, K_{AB} in the context of isentropic compression, denotes the energy of interaction between pairs of particles during the compression of the material. Similarly, the triplet interaction coefficient, K_{ABB} extends the concept of interaction to groups of three particles in the context of isentropic compression. Further information on this subject can be found in the works of Friedman and Krishan [42] and Franks et al. [43] for a more thorough comprehension. Pairwise interactions are important for the current study, as Table S1 demonstrates that the mixture of Asp + saccharide (s) + water has higher positive values for pair interaction coefficients than triplet interaction coefficients. Furthermore, compared to aqueous D-xylose, the pairwise interactions for the amino acid are more pronounced in aqueous L-arabinose.

Molecular separation (L_f)

Usually, when discussing a solution, the term molecular separation or intermolecular free length, L_f refers to the average distance between molecules. Jacobson's technique was used in accordance with Eq. (14) [44] to calculate L_f, and the results are displayed in Table 4.

$$L_f = kK_s^{1/2} \quad (14)$$

k is a temperature-dependent constant and is calculated as per the following relation (Eq. 15) [47].

$$k = (93.875 + 0.375T) \times 10^{-8} \quad (15)$$

The experimental temperature, T, for this study, is equal to 293.15 K, 298.15 K, 303.15 K, 308.15 K and 313.15 K.

In this instance, intra- and intermolecular interactions have a direct impact on the L_f values, which are associated with the isentropic compressibility values. The presence of hydrophilic groups $-OH$ and $-O-$ in saccharide (s) and $-NH_2$ and $-COOH$ in Asp is what causes the intermolecular and intramolecular interactions. Eyring's liquid state model explains the behavior and properties of liquids by considering molecular interactions and structures. According to this model, symmetrical systems tend to have low values of L_f. The parameter L_f is influenced by three key factors: symmetry, free volume, and molecular form. Symmetrical molecules are more uniform in shape and size, allowing them to pack more efficiently in a liquid state. This efficient packing reduces the available free volume and contributes to lower L_f values. Free volume refers to the space within the liquid that is not occupied by molecules. Thus, in symmetrical systems, the efficient packing of molecules leaves less free volume, further lowering L_f. The shape and structure of molecules also impact L_f. Symmetrical molecules tend to have simpler and more regular shapes, which facilitate efficient packing and minimize the free volume [45].

It can be observed from Table 4 that in an aqueous solution, Asp has lower values L_f, but in saccharides, L_f has higher values. The amino and hydroxyl functionalities in Asp and saccharides result in hydrogen-bonded big and symmetrical structures in solvents; when Asp concentration rises, L_f decreases in as per Eyring's liquid state modalities. Additionally, the presence of clathrate-like structures [46] traps the Asp molecules, creating incompressible structures that lower K_s and, in accordance with Eq. 5, lower L_f. L_f values fall as saccharide composition rises as well, suggesting enhanced amino acid-saccharide interaction. L_f values, on the other hand, rise with temperature, suggesting that the potential energy of interactions among the solute and solvent molecules decreases as the distance between them increases [47]. Furthermore, the trend towards decreasing free length suggests that the solute molecule is acting in a way that promotes structure. For a clear understanding of the variation of L_f with the concentration of Asp in aqueous L-arabinose/D-xylose at 298.15 K, a graphic representation is shown in figure S2.

Free volume (V_f) and internal pressure (π_i)

In a solution, the concept of "free volume" refers to the unoccupied space within the solvent where solute molecules can move freely. It represents the volume not occupied by solvent molecules or solute particles. Equation (16), which is the expression used for the evaluation of free volume, V_f,

Table 4 Values of internal pressure (π_i), relative ion association (R_A), acoustic impedance (Z), free length (L_f), free volume (V_f) and surface tension (γ) as functions of molality of Asp in water, aqueous L-arabinose/D-xylose media at 293.15 K, 298.15 K, 303.15 K, 308.15 K, 313.15 K and experimental pressure P = 101 kPa

Composition of solution	m/(mol kg^{-1})	$\pi_i \times 10^{-12}$/(N m^{-2})	$R_A \times 10^2$	$Z \times 10^{-5}$/(Kg m^{-2}s^{-1})	$L_f \times 10^{11}$/(m mol^{-1})	$V_f \times 10^9$ /(m^{3}mol^{-1})	$\gamma \times 10^2$/(Nm^{-1})
293.15 K							
Water	0.011	4.919	100.166	14.880	4.330	6.154	3.674
	0.019	4.928	100.150	14.910	4.324	6.174	3.683
	0.030	4.940	100.133	14.930	4.317	6.159	3.692
	0.039	4.945	100.118	14.950	4.313	6.138	3.698
	0.051	4.950	100.103	14.980	4.308	6.126	3.706
Aq L-arabinose 2.0 wt %	0.009	5.012	99.750	15.050	4.295	6.012	3.726
	0.021	5.020	99.764	15.070	4.289	5.998	3.734
	0.032	5.028	99.779	15.100	4.284	5.983	3.741
	0.040	5.038	99.794	15.120	4.278	5.969	3.749
	0.051	5.042	99.810	15.150	4.273	5.954	3.757
2.5 wt %	0.012	5.054	99.831	15.120	4.278	5.982	3.765
	0.021	5.062	99.844	15.150	4.272	5.966	3.765
	0.032	5.070	99.859	15.170	4.267	5.952	3.765
	0.042	5.080	99.873	15.190	4.261	5.937	3.765
	0.049	5.085	99.888	15.220	4.256	5.919	3.765
3.0 wt %	0.009	5.096	99.917	15.200	4.262	5.862	3.773
	0.022	5.104	99.932	15.220	4.257	5.846	3.780
	0.030	5.112	99.947	15.250	4.251	5.832	3.788
	0.039	5.122	99.962	15.270	4.246	5.815	3.796
	0.051	5.127	99.978	15.290	4.240	5.802	3.804
Aq D-xylose 2.0 wt %	0.012	5.005	99.748	15.040	4.298	6.044	3.722
	0.021	5.013	99.763	15.060	4.292	6.028	3.730
	0.032	5.021	99.777	15.090	4.286	6.014	3.738
	0.039	5.031	99.793	15.110	4.281	5.996	3.746
	0.052	5.036	99.808	15.140	4.275	5.979	3.754
2.5 wt %	0.009	5.040	99.758	15.110	4.281	5.982	3.746
	0.019	5.047	99.772	15.140	4.275	5.973	3.754
	0.031	5.053	99.788	15.160	4.269	5.964	3.761
	0.042	5.063	99.803	15.180	4.264	5.950	3.769
	0.049	5.070	99.82	15.210	4.258	5.921	3.777
3.0 wt %	0.012	5.073	99.819	15.180	4.266	5.872	3.767
	0.019	5.078	99.870	15.210	4.260	5.864	3.775
	0.028	5.081	99.919	15.230	4.255	5.851	3.783
	0.041	5.093	99.980	15.250	4.249	5.838	3.791
	0.050	5.100	100.04	15.280	4.244	5.824	3.799
298.15 K							
Water	0.011	5.095	100.103	14.950	4.345	7.030	3.704
	0.019	5.102	100.118	14.980	4.340	7.004	3.711
	0.030	5.114	100.133	15.000	4.334	6.988	3.721
	0.039	5.121	100.150	15.030	4.328	6.971	3.728
	0.051	5.127	100.166	15.050	4.323	6.953	3.736
Aq L-arabinose 2.0 wt %	0.009	5.102	99.748	15.040	4.335	7.004	3.724
	0.021	5.109	99.763	15.060	4.329	6.988	3.732
	0.032	5.115	99.777	15.090	4.323	6.965	3.739
	0.040	5.122	99.793	15.110	4.318	6.950	3.747
	0.051	5.130	99.808	15.140	4.312	6.934	3.755

Table 4 (continued)

Composition of solution	$m/(\text{mol kg}^{-1})$	$\pi_i \times 10^{-12}/(\text{N m}^{-2})$	$R_A \times 10^2$	$Z \times 10^{-5}/(\text{Kg m}^{-2}\text{s}^{-1})$	$L_f \times 10^{11}/(\text{m mol}^{-1})$	$V_f \times 10^9/(\text{m}^3\text{mol}^{-1})$	$\gamma \times 10^2/(N\text{m}^{-1})$
2.5 wt %	0.012	5.238	99.750	15.250	4.279	6.970	3.798
	0.021	5.246	99.764	15.270	4.274	6.947	3.806
	0.032	5.252	99.779	15.290	4.268	6.932	3.814
	0.042	5.259	99.794	15.320	4.263	6.909	3.822
	0.049	5.267	99.810	15.340	4.257	6.902	3.830
3.0 wt %	0.009	5.280	99.758	15.320	4.264	6.858	3.821
	0.022	5.287	99.772	15.350	4.259	6.843	3.829
	0.030	5.294	99.788	15.370	4.253	6.821	3.837
	0.039	5.300	99.803	15.390	4.248	6.799	3.845
	0.051	5.309	99.820	15.420	4.242	6.785	3.853
Aq D-xylose 2.0 wt %	0.012	5.187	99.719	15.160	4.300	7.010	3.770
	0.021	5.194	99.770	15.190	4.294	6.994	3.778
	0.032	5.200	99.819	15.210	4.288	6.979	3.786
	0.039	5.207	99.880	15.230	4.283	6.963	3.794
	0.052	5.215	99.940	15.260	4.277	6.940	3.802
2.5 wt %	0.009	5.213	99.731	15.220	4.285	6.992	3.790
	0.019	5.218	99.744	15.250	4.280	6.984	3.798
	0.031	5.224	99.759	15.270	4.274	6.976	3.806
	0.042	5.236	99.773	15.300	4.268	6.961	3.814
	0.049	5.243	99.788	15.320	4.263	6.930	3.822
3.0 wt %	0.012	5.256	99.840	15.310	4.268	6.874	3.816
	0.019	5.261	99.853	15.330	4.263	6.859	3.824
	0.028	5.263	99.866	15.350	4.257	6.845	3.832
	0.041	5.274	99.879	15.380	4.251	6.830	3.840
	0.050	5.281	99.894	15.400	4.246	6.815	3.848
303.15 K							
Water	0.011	5.273	99.964	15.022	4.361	7.823	3.733
	0.019	5.277	100.022	15.041	4.357	7.789	3.739
	0.030	5.289	100.067	15.069	4.351	7.768	3.748
	0.039	5.300	100.122	15.099	4.345	7.757	3.757
	0.051	5.305	100.179	15.123	4.339	7.735	3.765
Aq L-arabinose 2.0 wt %	0.009	5.300	99.916	15.195	4.327	7.867	3.785
	0.021	5.302	99.946	15.211	4.323	7.842	3.789
	0.032	5.309	99.959	15.234	4.318	7.821	3.797
	0.040	5.321	99.955	15.266	4.310	7.805	3.808
	0.051	5.329	99.969	15.289	4.304	7.785	3.816
2.5 wt %	0.012	5.344	99.753	15.265	4.310	7.800	3.808
	0.021	5.346	99.784	15.281	4.307	7.776	3.813
	0.032	5.352	99.798	15.304	4.301	7.756	3.821
	0.042	5.365	99.795	15.336	4.293	7.749	3.832
	0.049	5.373	99.810	15.360	4.288	7.729	3.840
3.0 wt %	0.009	5.390	99.926	15.346	4.294	7.687	3.833
	0.022	5.392	99.958	15.362	4.290	7.663	3.838
	0.030	5.399	99.972	15.385	4.285	7.644	3.845
	0.039	5.411	99.969	15.417	4.277	7.628	3.856
	0.051	5.419	99.984	15.441	4.271	7.618	3.864

Table 4 (continued)

Composition of solution	$m/(\text{mol kg}^{-1})$	$\pi_i \times 10^{-12}/(\text{N m}^{-2})$	$R_A \times 10^2$	$Z \times 10^{-5}/(\text{Kg m}^{-2}\text{s}^{-1})$	$L_f \times 10^{11}/(\text{m mol}^{-1})$	$V_f \times 10^9/(\text{m}^3\text{mol}^{-1})$	$\gamma \times 10^2/(N\text{m}^{-1})$
Aq D-xylose 2.0 wt %	0.012	5.294	99.890	15.185	4.329	7.863	3.781
	0.021	5.295	99.922	15.200	4.326	7.838	3.786
	0.032	5.302	99.938	15.224	4.320	7.814	3.794
	0.039	5.314	99.935	15.256	4.312	7.801	3.805
	0.052	5.322	99.950	15.280	4.307	7.781	3.813
2.5 wt %	0.009	5.326	99.874	15.255	4.313	7.795	3.804
	0.019	5.326	99.905	15.270	4.309	7.772	3.809
	0.031	5.332	99.921	15.294	4.304	7.752	3.817
	0.042	5.349	99.918	15.326	4.296	7.745	3.828
	0.049	5.357	99.933	15.350	4.290	7.723	3.836
3.0 wt %	0.012	5.365	99.909	15.331	4.297	7.683	3.827
	0.019	5.366	99.941	15.347	4.294	7.659	3.832
	0.028	5.367	99.957	15.371	4.288	7.640	3.840
	0.041	5.384	99.955	15.403	4.281	7.624	3.851
	0.050	5.392	99.971	15.427	4.275	7.615	3.859
308.15 K							
Water	0.011	5.473	99.815	15.115	4.370	8.783	3.771
	0.019	5.477	99.871	15.134	4.366	8.740	3.777
	0.030	5.481	99.939	15.153	4.363	8.720	3.782
	0.039	5.493	99.991	15.182	4.356	8.705	3.791
	0.051	5.499	100.051	15.207	4.351	8.688	3.799
Aq L-arabinose 2.0 wt %	0.009	5.458	99.917	15.266	4.341	8.763	3.822
	0.021	5.460	99.946	15.282	4.338	8.732	3.827
	0.032	5.467	99.960	15.305	4.333	8.717	3.834
	0.040	5.479	99.956	15.337	4.325	8.708	3.845
	0.051	5.487	99.970	15.360	4.319	8.681	3.853
2.5 wt %	0.012	5.488	99.899	15.334	4.325	8.748	3.837
	0.021	5.490	99.931	15.349	4.322	8.717	3.842
	0.032	5.497	99.944	15.373	4.316	8.690	3.850
	0.042	5.509	99.941	15.404	4.308	8.692	3.861
	0.049	5.518	99.955	15.428	4.303	8.666	3.869
3.0 wt %	0.009	5.530	99.927	15.403	4.310	8.697	3.859
	0.022	5.532	99.958	15.418	4.307	8.667	3.864
	0.030	5.539	99.972	15.442	4.302	8.641	3.872
	0.039	5.551	99.970	15.474	4.294	8.631	3.883
	0.051	5.559	99.985	15.497	4.288	8.617	3.891
Aq D-xylose 2.0 wt %	0.012	5.438	99.891	15.256	4.344	8.783	3.811
	0.021	5.440	99.924	15.271	4.341	8.763	3.816
	0.032	5.447	99.938	15.295	4.335	8.749	3.824
	0.039	5.459	99.937	15.327	4.327	8.727	3.835
	0.052	5.467	99.953	15.351	4.322	8.700	3.843
2.5 wt %	0.009	5.472	99.874	15.327	4.327	8.767	3.835
	0.019	5.472	99.905	15.343	4.324	8.748	3.840
	0.031	5.478	99.920	15.367	4.318	8.721	3.848
	0.042	5.496	99.918	15.398	4.310	8.699	3.859
	0.049	5.503	99.933	15.422	4.305	8.685	3.867

Table 4 (continued)

Composition of solution	m/(mol kg^{-1})	$\pi_i \times 10^{-12}$/(N m^{-2})	$R_A \times 10^2$	$Z \times 10^{-5}$/(Kg m^{-2}s^{-1})	$L_f \times 10^{11}$/(m mol^{-1})	$V_f \times 10^9$ /(m^{3}mol^{-1})	$\gamma \times 10^2$/(Nm^{-1})
3.0 wt %	0.012	5.505	99.910	15.388	4.314	8.749	3.854
	0.019	5.505	99.942	15.404	4.311	8.730	3.859
	0.028	5.506	99.957	15.428	4.305	8.716	3.867
	0.041	5.523	99.955	15.460	4.297	8.694	3.878
	0.050	5.531	99.971	15.484	4.292	8.668	3.886
313.15 K							
Water	0.011	5.639	99.819	15.157	4.393	9.777	3.790
	0.019	5.643	99.873	15.176	4.389	9.738	3.796
	0.030	5.648	99.941	15.194	4.386	9.727	3.801
	0.039	5.659	99.992	15.223	4.379	9.693	3.810
	0.051	5.665	100.048	15.247	4.374	9.686	3.818
Aq L-arabinose 2.0 wt %	0.009	5.592	99.917	15.338	4.356	9.709	3.845
	0.021	5.594	99.946	15.354	4.353	9.685	3.850
	0.032	5.601	99.959	15.377	4.347	9.652	3.858
	0.040	5.613	99.955	15.408	4.339	9.653	3.869
	0.051	5.622	99.970	15.432	4.334	9.620	3.877
2.5 wt %	0.012	5.640	99.900	15.412	4.339	9.659	3.870
	0.021	5.642	99.931	15.428	4.335	9.621	3.875
	0.032	5.649	99.945	15.451	4.330	9.602	3.883
	0.042	5.661	99.941	15.483	4.322	9.589	3.893
	0.049	5.670	99.957	15.507	4.316	9.571	3.901
3.0 wt %	0.009	5.684	99.927	15.485	4.323	9.610	3.892
	0.022	5.686	99.958	15.500	4.320	9.572	3.897
	0.030	5.693	99.972	15.524	4.315	9.554	3.905
	0.039	5.705	99.969	15.556	4.307	9.541	3.916
	0.051	5.714	99.985	15.579	4.301	9.523	3.924
Aq D-xylose 2.0 wt %	0.012	5.585	99.891	15.328	4.358	9.734	3.841
	0.021	5.587	99.924	15.343	4.355	9.709	3.846
	0.032	5.594	99.939	15.367	4.349	9.690	3.854
	0.039	5.607	99.938	15.399	4.342	9.676	3.865
	0.052	5.615	99.954	15.423	4.336	9.643	3.873
2.5 wt %	0.009	5.621	99.875	15.401	4.341	9.683	3.866
	0.019	5.621	99.907	15.417	4.338	9.659	3.871
	0.031	5.627	99.922	15.440	4.332	9.640	3.879
	0.042	5.645	99.920	15.472	4.325	9.612	3.890
	0.049	5.653	99.935	15.496	4.319	9.594	3.898
3.0 wt %	0.012	5.658	99.910	15.470	4.327	9.660	3.887
	0.019	5.658	99.942	15.486	4.324	9.650	3.892
	0.028	5.660	99.957	15.510	4.318	9.617	3.900
	0.041	5.677	99.955	15.541	4.310	9.604	3.911
	0.050	5.685	99.970	15.565	4.305	9.571	3.919

Standard uncertainties: u(m_A) = 1 × 10^{-3}mol kg^{-1}(with a confidence level of 0.68). u (wt %) = ± 0.05 wt %, u (T) = 0.01 K, u(p) = 1.0 kPa

$$V_f = \left\{ \left(\bar{M}U/(k \times \eta) \right\}^{3/2} \quad (16)$$

$\bar{M}$ The average molar mass (m) of the solution can be computed using the Eq. (17) that follows [48]

$$\bar{M} = \sum_{i=1}^{3} x_i M_i \tag{17}$$

A value of 4.28×10^9 is assigned to the temperature-independent constant term k, whereas η represents the dynamic viscosity of the solutions being studied, whose obtained values in N s m^2 are converted into Kgm^{-1} s^{-1} [24] and are recorded in Table 2. According to the average free volume concept, hard-core spheres of solvated particles arise as a result of strong attraction forces between solute and solvent molecules. As stronger interactions are anticipated at higher solute and cosolute concentrations, the solvation spheres shrink in volume and fit neatly inside the solvent's interstitial spaces. As a result, as seen in Table 4, the free volume decreases when Asp and saccharide (s) content ascend. The solute–solvent interaction is more prominent in the Asp and aqueous saccharide systems, according to the results of adiabatic compressibility and intermolecular free path length, which were found to decrease with concentration and increase with temperature, whereas ultrasonic velocity and viscosity were found to increase with concentration and increase with temperature. This was further confirmed by the analysis of another important acoustic parameter, i.e. internal pressure. The outcome of the forces of attraction and repulsion between molecules in the interior of the solution is the internal pressure *(π_i)*. π_i can be deduced using the Eq. (18) given below,

$$\pi_i = (\alpha T / K_T) - P \tag{18}$$

Table 4 lists the values of π_i. The experiment was conducted at atmospheric pressure (P), which is not taken into account in the calculations that are shown.

Associative solute–solvent interactions put structural and chemical pressure on the solute. The internal pressure of a solution thus increases above that of a pure solvent. Strong, cohesive contacts between the polar groups of Asp, saccharides, and the ionic components at increasing concentrations promote the clustering process, which causes internal pressure to rise with concentration. Table 4 illustrates that in both aqueous L-arabinose and aqueous D-xylose systems, free volume dropped and internal pressure rose for Asp. Once more, this supported the notion that interactions between solutes and solvents exist in the system under study.

Relative association (R_A)

In the context of solutions, it often refers to the tendency of solute molecules to associate with each other or with solvent molecules, altering their behaviour compared to what would be expected based solely on their individual properties. In other words, a crucial acoustical characteristic that sheds light on the kinds of interactions that occur between like-like and unlike parts is relative association, or R_A. It provides insight into the degree of correlation that exists among the constituents. The densities and sound velocities of solutions and solvents are employed in accordance with the following relation (Eq. 19) to evaluate the R_A parameter [49].

$$R_A = (\rho/\rho_o) \times (U_0/U)^{1/3} \tag{19}$$

In Table 4, we saw an increasing trend in R_A variation with Asp and saccharide (s) concentrations. In the context of ion-ion and ion-hydrophilic attractive forces between $-NH_3^+$ and $-COO^-$ on the Asp chain ends, polar parts of saccharides and the polar water molecules, an explanation of this trend has been put forth. Two things affect the R_A values: (i) the solute molecules' hydration; (ii) The molecules of the solute break the solvent's structure. Component (i) raises the R_A values, whereas component (ii) lowers them. Table 4 demonstrates that for binary and ternary Asp solutions, the hydration of solute molecules dominates over the solvent structure breaking with an increase in solute concentration at both temperatures. An increase in R_A values with an increase in Asp concentration for each composition of saccharides under investigation suggests the presence of significant interionic and solute–solvent interactions. That is the values of R_A increase with an increase in the composition of L-arabinose/D-xylose, suggesting a strong interaction between the amino acids and saccharides. As the temperature increases, the interionic attraction between the solute and solvent molecules weakens. This means that the forces holding the solute ions and solvent molecules together become less strong. This weakening of attraction is reflected in the decrease in the R_A values (a parameter that indicates the strength of these interactions) as the temperature rises. In simpler terms, higher temperatures reduce the strength of the interaction between solute and solvent molecules, which is evidenced by the lower R_A values observed at elevated temperatures.

Acoustic impedance (Z)

Using density (ρ) and ultrasonic velocity (U) data, the acoustic impedance (Z) has been calculated (Eq. 20) [50]. It is the medium's resistance to the motion of the longitudinal waves. The more molecules interact with one another, the stronger the opposition will be, raising the values. The Table 4 for Z values of each system makes this clear.

$$Z = \rho \times U \tag{20}$$

The ratio of the effective sound pressure on a particle in the medium to the effective particle velocity is typically used to determine the medium's acoustic impedance (Z). When a sound wave travels through a medium, its inertial and elastic qualities cause various medium particles to experience varying sound pressures. Therefore, the total rise in Z values can be attributed to an increase in the effective sound pressure at any given solution molecule. The Z values in the systems under investigation have increased due to the rise in solute (Asp) and co-solute (L-arabinose/D-xylose) concentrations (Table 4). This suggests that the solvent and solute molecules have strong molecular interactions. A visual depiction is given in figure S3 for a comprehensive grasp on the variation in Z values with a change in concentration of Asp in different compositions of saccharides at 298.15 K. The stronger cohesive molecular connections are predicted as the solution's concentration rises. Sound waves travel by vibrating particles in a medium (like air, water, or a solid). The closer the particles are packed together, the more efficiently the sound can travel through that medium. Impedance in this context is a measure of how much the medium resists the passage of sound waves. When particles are closely packed (denser media), sound waves encounter more resistance because there are more particles to vibrate. When solute (like salt) or cosolutes (another substance) is added to a solution, it increases the density of the solution because the added molecules fill in the spaces between the solvent molecules (like water). Hence, when the concentration of solutes or cosolutes is increased, the medium becomes denser, thereby increasing the impedance (Z value) because there are more particles for the sound waves to interact with [51]. Stereochemistry deals with the 3D arrangement of atoms in molecules. L-arabinose and D-xylose, despite being similar sugars, have different spatial arrangements. This affects how they interact with other molecules, including Asp. A number of studies have emphasized the critical function that the spatial orientation of the $-OH$ group at C4 plays in the interactions between proteins and molecular ligands as well as carbohydrates. The interactions between Asp and certain isomeric monosaccharides (D-glucose, D-galactose, and Dfructose) in aqueous solution are investigated by G. A. Kulikova et al. following densimetry, calorimetry of dissolution and isothermal titration calorimetry approach. It was observed that the axial orientation of the $-OH$ group at C4 in D-galactose molecule prevented the establishment of the interaction between this monosaccharide and Asp [40]. D-xylose fits better into the water structure, meaning it forms more stable interactions with water molecules. Because of this, D-xylose is less available to interact with the polar sites on Asp. L-arabinose doesn't fit into the water structure as well as D-xylose does. For the current study, it can be observed that Z values are higher for Asp in aqueous L-arabinose than aqueous D-xylose (Table 4). This means L-arabinose is more available to interact with Asp's polar sites, leading to stronger interactions and higher Z values in the solution [1, 2]. Thus, the molecular packing of the medium [52], the molecular structure of the particles, the solvation process, the caging effect of the solvent, and the solute's structure-making/breaking properties all affect the pattern of sound waves. Pressure changes from one particle to another, which happens as a sound wave passes through a medium. The medium's elastic quality is a key component that controls this aspect.

Surface tension (γ)

A physical characteristic of matter, surface tension, or σ, is connected to the potential energy of intermolecular interactions and the liquid interfacial microstructure [53]. At low and moderate temperatures and pressures, the surface tension can be measured with excellent accuracy; at high temperatures and pressures, computer simulations are used to determine the values [54]. As a result of molecules moving more quickly at higher temperatures, which diminishes cohesive forces, surface tension typically decreases with temperature. On the other hand, as the temperature rose in the current investigation, surface tension increased. Although it's not common, there are instances in which surface tension rises with temperature; these are less common and often happen with particular compounds or under particular conditions. The variability can be attributed to a number of reasons, including (i) particular molecular interactions, (ii) temperature-dependent structural changes, (iii) the degree of non-ideality, etc. Saccharides are the fundamental family of chemicals due to their hydrophilic hydroxyl ($-OH$) groups, homochirality, stereoselectivity, and coordinating abilities. Every sugar that is crystalline-free has a distinct stereoisomer. Many sugars, like L-arabinose and D-xylose, can form a ring structure known as a hemiacetal. This ring can open and close when the sugar dissolves in water. The opening and closing of the sugar rings in water (mutarotation) leads to multiple ring structures of different shapes and sizes at a specific carbon atom called the anomeric center. Due to mutarotation, L-arabinose and D-xylose exhibit various potential structures in water. They don't just stay in one form but constantly switch between multiple forms. Less than 1% of reducing monosaccharides are found in the acyclic state in solution. Most of them exist in cyclic (ring) forms. These sugars exist in a dynamic balance between their cyclic and acyclic forms. The dynamic nature of sugars like L-arabinose and D-xylose in water,

due to mutarotation and the balance between cyclic and acyclic forms, leads to variations in intermolecular interactions. These variations influence the arrangement of molecules at the liquid's surface, ultimately affecting the surface tension. It is seen from Table 4 that surface tension rose as temperature increased. This may be due to the strong intermolecular interactions that occur between L-arabinose/D-xylose and Asp's polar sites in aqueous conditions.

The initial drop in surface tension when introducing a small amount of solute is due to the disruption of the uniform solvent–solvent interactions at the surface, which reduces the cohesive forces among the solvent molecules. This makes it easier to increase the surface area of the liquid, hence the lower surface tension. Because of the creation of aggregates or intricate structures at the surface, increased solute concentration might result in strong solute–solvent interactions and potentially raise surface tension. With concentration, these intricate structures have the ability to change the surface's characteristics and cause surface tension to increase [55]. The surface tension increasing as the amount of Asp in the solution increases (Table 4) reveals this. Along with the rise in saccharide composition in the aqueous medium, the surface tension values also rose. The increased surface tension data for aqueous L-arabinose across all compositions lends additional credence to the idea that Asp interacts with L-arabinose more frequently than D-xylose. Xueli Zhou et al. reported the surface tension data for *N*, *N*-diethylethanolamine (DEEA) in aqueous 2-amino-2-methyl-1-propanol (AMP)/piperazine (PZ). Surface tension values for pure components decreased with temperature in all systems under study, following the order H2O>AMP/PZ>DEEA. The surface tension values are nearly in the same range as in the current study [56]. The literature also reports, with increase in amino alcohol (monoethanolamine (MEA)/2-Amino-2-methyl-1-propanol (AMP)) concentration in aqueous medium surface tension gets increased. However, the alteration in surface tension due to a specific variation in alkanolamine concentration is more pronounced at lower concentrations compared to higher concentrations [57].

FTIR spectral analysis

An additional crucial tool that offers details on the interactions between various groups is FTIR spectroscopy. It depends on the vibrations of the atoms within a molecule. These vibrations give insight into the chemical interactions within the system [58]. The FTIR spectra of Asp in a 2.0 wt % aqueous solution of L-arabinose or D-xylose were recorded in the range of wavenumbers from 4000 cm^{-1} to 400 cm^{-1}. One major peak appears in all the spectral data, corresponding to the *O–H* stretching band. This is a characteristic absorption due to the vibration of *O–H* bonds (like those in water or alcohol groups). Between 1625 cm^{-1} and 1660 cm^{-1}, a distinct stretching band is observed for the aliphatic carboxylic groups (> C = O) in all amino acid solutions. This corresponds to the carbonyl group vibrations in the amino acid. The absorption peaks between 3300 cm^{-1} and 3650 cm^{-1} are sensitive to hydrogen bonding. They correspond to *O–H* and N–H stretching vibrations. When molecules form hydrogen bonds, these vibrations shift, indicating changes in the molecular environment. The broad absorption band shifts due to intermolecular hydrogen bonding, suggesting ion-hydrophilic (water-attracting) or hydrophobic (water-repelling) interactions in the solution. This means that the interactions between different parts of the molecules are changing the way they vibrate and absorb IR light. As the concentration of Aspartic acid in the solution increases, there is more hydrogen bonding between water molecules and the polar groups $\left(NH_3^+, COO^-\right)$ of the amino acid [59, 60]. This increased hydrogen bonding causes O–H and N–H stretching bands to shift to a lower frequency in the IR spectrum. Lower frequency means that the bonds are more relaxed or stretched due to the interactions [61]. It signifies that the H-bonded network of water by Asp is strengthened by the presence of L-arabinose and D-xylose. So it may be interpreted that a change in concentration of amino acid causes a shift in wave numbers, which indicates some structural changes, which are also predicted from the acoustic study. A graphic representation of the spectra of Asp in pure water and aqueous L-arabinose/D-xylose (2.0 wt % composition) is displayed in Fig. 4.

Based on acoustic and FTIR studies, as well as thermodynamic analysis and transfer parameters from the volumetric and viscometric study that was recently published [2],this study challenges that molecular interactions of the types hydrophilic-hydrophilic and hydrophilic-ionic are easily observed and efficient among the axial and equatorial −OH groups of L-arabinose/D-xylose, and the zwitterions of Asp in water. Temperature-dependent changes in the strength or extent of these connections among Asp and L-arabinose/D-xylose affect the solution's overall stability and behaviour. Therefore, the system being studied and the methodology selected provide a fresh viewpoint, allowing for the prediction of interaction patterns or complexes that may not be easily detectable through experimental methods. These insights go beyond what traditional experimental methods might capture, offering a deeper understanding of the system's behaviour. In addition, the present work investigates these interactions emphasizing the thermodynamic and structural differences between

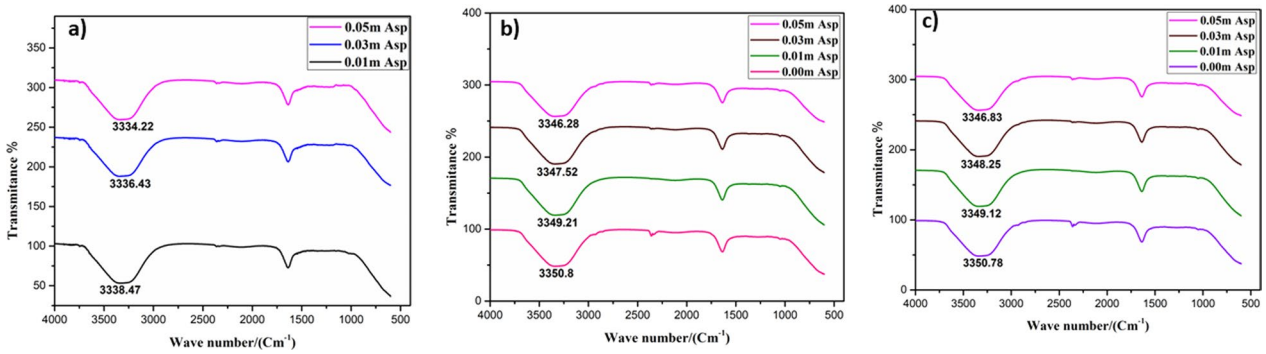

Fig. 4 Asp's FTIR spectra in (**a**) water, (**b**) 2.0 weight percent aqueous L-arabinose, and (**c**) 2.0 weight percent D-xylose

Asp and Glu in saccharide-rich environments. By employing similar physicochemical and spectroscopic techniques, this study enables a comparative analysis that builds upon the findings of the earlier work.

Conclusions

The current investigation has examined the degree of molecular interaction between the solute (Asp), co-solute (L-arabinose/D-xylose), and solvent (water) using acoustic and spectroscopic methods and their characteristics at five distinct temperatures (293.15 K to 313.15 K). Increased ultrasonic velocity is the result of stronger particle interactions caused by higher concentrations of Asp and L-arabinose/D-xylose. The decreasing trends in compressibility metrics (K_s, K_T and $K_{s,\phi}$) with concentration suggest that bulk water molecules are much more compressible than the electrostricted water molecules in the hydration shells around Asp and the polar regions of saccharides. In evaluated solutions, positive values of $K^0_{s,\phi,\,tr}$ indicate Asp's structure-making activity. Its pair and triplet interaction coefficient indicates that Asp has more pairwise interactions with water + L-arabinose than with watery D-xylose. The increase in acoustic impedance (Z), internal pressure (π_i), relative association (R_A), surface tension (γ), and decrease in free volume (V_f) and free length (L_f) reveal that the interactions between hydrophilic parts and ions are stronger than those between hydrophobic moities. L-arabinose molecules'axial-equatorial $-OH$ groups prefer to bind with Asp molecules over D-xylose's equatorial $-OH$ groups. FTIR analysis reveals that Asp strengthens the H-bonded network of water in the presence of L-arabinose and D-xylose by shifting the $-O-H$ and $-N-H$ stretching bands to a lower frequency range. Further studies on different saccharides and amino acids are strongly advised, with consideration given to factors like mutarotation, anomeric effect, solubility and stereochemistry of saccharides, which affect how the different moieties interact with one another in the solution. The results of this investigation can be utilized to quantitatively investigate the interactions between Asp and L-arabinose/D-xylose. Using the FTIR spectroscopy analysis, the chemical structures and functional groups involved in interactions can be further examined. Experimental results can be enhanced by computational methods like quantum chemistry computations and molecular dynamics simulations. research offers exciting future prospects across various fields. It can contribute significantly to drug design by providing insights into saccharide-based therapeutics and efficient drug delivery systems. The findings on molecular interaction may also advance biotechnology by aiding in the development of biocompatible materials and enhancing enzymatic processes involving amino acids and saccharides. In nutritional science, this study could inspire innovations in dietary supplements and functional food formulations. Additionally, the research has potential applications in material science for creating advanced biomaterials tailored for medical and industrial uses.

Supplementary Information

The online version contains supplementary material available at https://doi.org/10.1186/s13065-025-01490-6.

Supplementary Material 1

Acknowledgements

We express our sincere gratitude to the Department of Chemistry at ITER, Siksha O Anusandhan Deemed to be University, for providing the essential facilities that enabled us to complete the experimental work presented in this article.

Author contributions
RKP: Experimentation, conception and design of the data; prepared all figures; SS: analysis and interpretation of the data, drafting the article or revising it critically for important intellectual content; guided to wrote the main manuscript text, approval of the final version.

Funding
Open access funding provided by Siksha 'O' Anusandhan (Deemed To Be University).

Availability of data and materials
The data supporting this article have been included as part of the Supplementary Information.

Declarations

Ethics approval and consent to participate
Not applicable.

Consent for publication
Not applicable.

Competing interests
The authors declare no competing interests.

Author details
[1]Department of Chemistry, ITER, Siksha O Anusandhan Deemed to be University, Bhubaneswar, Odisha, India.

Received: 24 January 2025 Accepted: 25 April 2025
Published online: 19 May 2025

References

1. Kumar Pradhan R, Sahoo L, Singh S. Volumetric and viscometric properties of L-glutamic acid in aqueous L-arabinose and D-xylose solutions between the temperature range of (293.15–313.15) K at atmospheric pressure. J Chem Thermodyn. 2024;189: 107193. https://doi.org/10.1016/j.jct.2023.107193.
2. Kumar Pradhan R, Singh S. Exploration of interactions between L-aspartic acid and saccharides in aqueous medium at T = (293.15–313.15) K: physicochemical and spectroscopic approach. J Mol Liq. 2024;394: 123788. https://doi.org/10.1016/j.molliq.2023.123788.
3. Pradhan RK, Singh S. Exploring the effects of saccharides on the solvation behaviour of L-Citrulline in aqueous medium: volumetric, transition state theory, transfer parameters and spectroscopic approach. Food Chem. 2024;452: 139554. https://doi.org/10.1016/j.foodchem.2024.139554.
4. Mohapatra P, Mohapatra S, Panda MP, Mishra C, Singh S, Talukdar M. Probing into volumetric and acoustic properties of aqueous L-ascorbic acid in the presence of diammonium hydrogen phosphate and potassium chloride. J Chem Eng Data. 2024. https://doi.org/10.1021/acs.jced.4c00394.
5. Talukdar M, Dey S, Panda A, Pan S, Singh S. Exploring the effect of ammonium acetate on volumetric, viscometric and conductive properties of L-aspartic acid in aqueous medium at different temperatures. J Solution Chem. 2024;53:387–415. https://doi.org/10.1007/s10953-023-01335-7.
6. Pradhan RK, Singh S. Studies on interactions of L-glutamic acid with L-arabinose/D-xylose in aqueous medium: ultrasonic velocity and acoustic parameter studies supported by FTIR spectroscopic investigation. J Mol Liq. 2024;412: 125790. https://doi.org/10.1016/j.molliq.2024.125790.
7. Banipal TS, Kaur J, Banipal PK, Sood AK, Singh K. Volumetric and viscometric studies of some amino acids in aqueous solutions of cadmium chloride at T = (288.15 to 318.15) K and at atmospheric pressure. J Chem Eng Data. 2011;56:2751–60. https://doi.org/10.1021/je100909b.
8. Jiang X, Zhu C, Ma Y. Volumetric and viscometric studies of amino acids in l-ascorbic acid aqueous solutions at T=(293.15 to 323.15)K. J Chem Thermodyn. 2014;71:50–63. https://doi.org/10.1016/j.jct.2013.11.002.
9. Bobicz D, Grzybkowski W, Lewandowski A. Apparent molar volumes of divalent transition metal chlorides and perchlorates in dimethyl sulfoxide solutions. J Mol Liq. 2003;105:93–104. https://doi.org/10.1016/S0167-7322(03)00015-1.
10. Ankita AK. Nain, Study of solvation behaviour and interactions of drug betaine hydrochloride in aqueous-D-xylose/L-arabinose solutions at different temperatures by using volumetric, acoustic and viscometric methods. J Chem Thermodyn. 2020;143: 106046. https://doi.org/10.1016/j.jct.2019.106046.
11. Zhao C, Ma P, Li J. Partial molar volumes and viscosity B-coefficients of arginine in aqueous glucose, sucrose and l-ascorbic acid solutions at T=298.15 K. J Chem Thermodyn. 2005;37:37–42. https://doi.org/10.1016/j.jct.2004.07.030.
12. Zhuo K, Liu Q, Wang Y, Ren Q, Wang J. Volumetric and viscosity properties of monosaccharides in aqueous amino acid solutions at 298.15 K. J Chem Eng Data. 2006;51:919–27. https://doi.org/10.1021/je050412t.
13. Millero FJ, Lo Surdo A, Shin C. The apparent molal volumes and adiabatic compressibilities of aqueous amino acids at 25.degree.C. J Phys Chem. 1978;82:784–92. https://doi.org/10.1021/j100496a007.
14. Lee JC, Timasheff SN. The stabilization of proteins by sucrose. J Biol Chem. 1981;256:7193–201. https://doi.org/10.1016/S0021-9258(19)68947-7.
15. Fágáin CÓ. Understanding and increasing protein stability. Biochim Biophys Acta Protein Struct Mol Enzymol. 1995;1252:1–14. https://doi.org/10.1016/0167-4838(95)00133-F.
16. Dhal K, Singh S, Talukdar M. Elucidation of molecular interactions of aspartic acid with aqueous potassium sorbate and sodium benzoate: volumetric, viscometric and FTIR spectroscopic investigation. J Mol Liq. 2022;352: 118659. https://doi.org/10.1016/j.molliq.2022.118659.
17. Kumar I, Lomesh SK, Singh D, Kumar P, Ahir P, Kumar S. Volumetric, ultrasonic, conductometric and UV–visible analysis of molecular interactions between metformin hydrochloride and dulcitol in aqueous solutions. J Mol Liq. 2024;396: 124089. https://doi.org/10.1016/j.molliq.2024.124089.
18. Mohapatra P, Singh S, Talukdar M. Analysis of viscometric and conductometric properties of L-ascorbic acid in aqueous potassium chloride and diammonium hydrogen phosphate. J Chem Eng Data. 2024. https://doi.org/10.1021/acs.jced.4c00350.
19. Ali A, Tariq M. Surface thermodynamic behaviour of binary liquid mixtures of benzene + 1,1,2,2-tetrachloroethane at different temperatures: an experimental and theoretical study. Phys Chem Liq. 2008;46:47–58. https://doi.org/10.1080/00319100701344628.
20. Dhal K, Das P, Singh S, Talukdar M. Analysis of ultraacoustic behavior of l-aspartic acid in aqueous sodium benzoate and ammonium acetate media. J Mol Liq. 2023;376: 121413. https://doi.org/10.1016/j.molliq.2023.121413.
21. Jamal MA, Naseem B, Khosa MK, Muneer M, Khan JH. Effect of anionic micellar medium on thermo-acoustical parameters of aspartic acid and serine solutions. J Mol Liq. 2017;237:14–22. https://doi.org/10.1016/j.molliq.2017.04.073.
22. Gaba R, Pal A, Sharma D, Kumar H, Kumar A. Molecular interactions of some non-essential amino acids in aqueous solutions of 1-methylimidazolium chloride at different temperatures. J Mol Liq. 2019;279:711–8. https://doi.org/10.1016/j.molliq.2019.01.094.
23. Singh H, Richu, Bandral A, Majid Q, Kumar A. Investigation of molecular interactions of streptomycin sulphate with aqueous L-aspartic acid through volumetric, ultrasonic and viscometric approach. J Mol Liq. 2023;382: 121885. https://doi.org/10.1016/j.molliq.2023.121885.
24. Nain AK. Insight into solute-solute and solute-solvent interactions of l-proline in aqueous-D-xylose/L-arabinose solutions by using physicochemical methods at temperatures from 293.15 to 318.15 K. J Mol Liq. 2020;318: 114190. https://doi.org/10.1016/j.molliq.2020.114190.
25. Kaur H, Chakraborty N, Juglan KC, Upmanyu A. Thermodynamic and physicochemical characteristics of 2-butoxyethanol/2-phenoxyethanol in aqueous maltitol solutions. J Mol Liq. 2023;392: 123403. https://doi.org/10.1016/j.molliq.2023.123403.
26. Zhuo K, Wang J, Wang H. Activity coefficients for NaCl–monosaccharide (d-glucose, d-galactose, d-xylose, d-arabinose)–water systems at 298.15 K. Carbohydr Res. 2000;325:46–55. https://doi.org/10.1016/S0008-6215(99)00298-0.
27. Bankar ST, Khaty NT, Umredkar PY, Ganorkar KS, Khaty RN, Dhondge SS, Tangde VM. Thermodynamic characterization of aqueous solutions of NaCl, KCl, MgCl2 and CaCl2: volumetric, acoustic, viscometric and computational analysis. J Mol Liq. 2024;393: 123670. https://doi.org/10.1016/j.molliq.2023.123670.

28. Borović TT, Panić J, Radović I, Grozdanić N, Vraneš M. Interactions of caffeine and 1-butyl-3-methylimidazolium salicylate ionic liquid in water—solubility, volumetric, acoustic, viscometric and refractometric studies supported by MD simulation. J Mol Liq. 2024;397: 124058. https://doi.org/10.1016/j.molliq.2024.124058.
29. Zafarani-Moattar MT, Sarmad S. Effect of tri-potassium phosphate on volumetric, acoustic, and transport behaviour of aqueous solutions of 1-ethyl-3-methylimidazolium bromide at T=(298.15 to 318.15)K. J Chem Thermodyn. 2010;42:1213–21. https://doi.org/10.1016/j.jct.2010.04.025.
30. Pandey JD, Sanguri V, Yadav MK, Singh A. Intermolecular free length and free volume of pure liquids at varying temperatures and pressures. Indian J Chem. 2008;47A:1020–5.
31. Ahmad Sajid T, Jamal MA, Saeed M, Atta-ul-Haq, Muneer M. Elucidation of molecular interactions between amino acid and imidazolium based ionic liquid in an aqueous system: volumetric and acoustic studies. J Mol Liq. 2021;335: 116513. https://doi.org/10.1016/j.molliq.2021.116513.
32. Asghar Jamal M, Sohail A, Muneer M, Abbas G, Shah S, Ahmad Sajid T. Volumetric-acoustic investigations of antihypertensive drug in aqueous acetaminophen system. J Mol Liq. 2024;398: 124331. https://doi.org/10.1016/j.molliq.2024.124331.
33. Rajput P, Singh H, Kumar A. Volumetric, ultrasonic and viscometric behavior of nucleosides (uridine and cytidine) in aqueous L-ascorbic acid solutions at different temperatures. J Chem Thermodyn. 2022;171: 106805. https://doi.org/10.1016/j.jct.2022.106805.
34. Keshapolla D, Gardas RL. Apparent molar volumes and isentropic compressions of benzylalkylammonium ionic liquids in dimethylsulfoxide from 293.15 K to 328.15 K. Fluid Phase Equilib. 2014;383:32–42. https://doi.org/10.1016/j.fluid.2014.09.022.
35. Kirkwood JG. Theoretical studies upon dipolar ions. Chem Rev. 1939;24:233–51. https://doi.org/10.1021/cr60078a004.
36. Yan Z, Wang J, Kong W, Lu J. Effect of temperature on volumetric and viscosity properties of some α-amino acids in aqueous calcium chloride solutions. Fluid Phase Equilib. 2004;215:143–50. https://doi.org/10.1016/j.fluid.2003.07.001.
37. Liu H, Lin R, Zhang H. Enthalpic interactions of amino acids with saccharides in aqueous solutions at 298.15 K. J Chem Eng Data. 2004;49:416–20. https://doi.org/10.1021/je030227k.
38. Sadeghi R, Ziamajidi F. Apparent Molar volume and isentropic compressibility of trisodium citrate in water and in aqueous solutions of polyvinylpyrrolidone at T = (283.15 to 308.15) K. J Chem Eng Data. 2007;52:1037–44. https://doi.org/10.1021/je700001x.
39. Singh V, Chhotaray PK, Gardas RL. Effect of protic ionic liquid on the volumetric properties and taste behaviour of sucrose. Food Chem. 2015;169:478–83. https://doi.org/10.1016/j.foodchem.2014.08.023.
40. Kulikova GA, Parfenyuk EV. Interaction between some monosaccharides and aspartic acid in dilute aqueous solutions. J Biol Phys. 2007;33:247–54. https://doi.org/10.1007/s10867-008-9057-4.
41. McMillan WG, Mayer JE. The statistical thermodynamics of multicomponent systems. J Chem Phys. 1945;13:276–305. https://doi.org/10.1063/1.1724036.
42. Krishnan CV, Friedman HL. Enthalpies of alkyl sulfonates in water, heavy water, and water-alcohol mixtures and the interaction of water with methylene groups. J Solution Chem. 1973;2:37–51. https://doi.org/10.1007/BF00645870.
43. Franks F, Pedley M, Reid DS. Solute interactions in dilute aqueous solutions Part 1—Microcalorimetric study of the hydrophobic interaction. J Chem Soc Faraday Trans 1 Phys Chem Condens Phases. 1976;72:359. https://doi.org/10.1039/f19767200359.
44. Pandey JD, Dey R, Chhabra J. Thermoacoustical approach to the intermolecular free-length of liquid mixtures. PhysChemComm. 2003;6:55. https://doi.org/10.1039/b307435h.
45. Pandey JD, Kumar V, Saxena MC. Evaluation of Jacobson's constant and intermolecular free-length as a function of pressure and temperature for cryogenic liquids. Ultrasonics. 1979;17:153–8. https://doi.org/10.1016/0041-624X(79)90032-5.
46. Rao NP, Verrall RE. Ultrasonic velocity, excess adiabatic compressibility, apparent molar volume, and apparent molar compressibility properties of binary liquid mixtures containing 2-butoxyethanol. Can J Chem. 1987;65:810–6. https://doi.org/10.1139/v87-137.
47. Asghar Jamal M, Naseem B, Naz S, Arif I, Saeed M, Atiq S. Thermo-acoustic properties of maltose in aqueous amino acids system. J Mol Liq. 2020;309: 112932. https://doi.org/10.1016/j.molliq.2020.112932.
48. Affandi MMR, Tripathy M, Majeed ABA. Solubility enhancement of simvastatin and atorvastatin by arginine: a solvodynamics study. J Mol Liq. 2017;241:359–66. https://doi.org/10.1016/j.molliq.2017.05.003.
49. Naseem B, Iftikhar M. Investigation on molecular interactions of antibiotics in alcohols using volumetric and acoustic studies at different temperatures. J Chem Thermodyn. 2017;104:239–51. https://doi.org/10.1016/j.jct.2016.09.037.
50. Lomesh SK, Kumar D. Volumetric, viscosity and ultrasonic studies of solute-solute and solute-solvent interactions of glycine and diglycine in water and in aqueous citric acid at different temperatures. J Mol Liq. 2017;241:764–71. https://doi.org/10.1016/j.molliq.2017.05.004.
51. Nori TS, Babavali SKF, Srinivasu C, Narendra K. FTIR spectroscopic studies with thermo acoustical parameters in binary liquid mixtures at different temperatures. J Mol Liq. 2019;287: 110944. https://doi.org/10.1016/j.molliq.2019.110944.
52. Chauhan S, Sharma K. Extended studies on molecular interactions of SDBS and DTAB in aqueous solutions of amino acid at T=293.15–313.15K. J Mol Liq. 2015;211:675–85. https://doi.org/10.1016/j.molliq.2015.08.003.
53. Irving JH, Kirkwood JG. The statistical mechanical theory of transport processes. IV. The equations of hydrodynamics. J Chem Phys. 1950;18:817–29. https://doi.org/10.1063/1.1747782.
54. Biscay F, Ghoufi A, Lachet V, Malfreyt P. Prediction of the surface tension of the liquid–vapor interface of alcohols from monte carlo simulations. J Phys Chem C. 2011;115:8670–83. https://doi.org/10.1021/jp1117213.
55. Oroian M, Ropciuc S, Amariei S, Gutt G. Correlations between density, viscosity, surface tension and ultrasonic velocity of different mono- and di-saccharides. J Mol Liq. 2015;207:145–51. https://doi.org/10.1016/j.molliq.2015.03.033.
56. Zhou X, Song Q, Chen Y, Yang F. Surface tension measurement and modeling for ternary aqueous solutions of N, N-diethylethanolamine + 2-amino-2-methyl-1-propanol/piperazine + water at T = (293.15 to 318.15) K. J Chem Thermodyn. 2025;201: 107405. https://doi.org/10.1016/j.jct.2024.107405.
57. Vázquez G, Alvarez E, Navaza JM, Rendo R, Romero E. Surface tension of binary mixtures of water + monoethanolamine and water + 2-amino-2-methyl-1-propanol and tertiary mixtures of these amines with water from 25 °C to 50 °C. J Chem Eng Data. 1997;42:57–9. https://doi.org/10.1021/je960238w.
58. Kumar H, Katal A. Volumetric, acoustic and spectroscopic studies (FT-IR) of trisodium (TSC) and tripotassium citrate (TPC) in aqueous solution of ionic liquid 1-butyl-3-methylimidazolium tetrafluoro borate [C 4 mim][BF 4] at different temperatures. J Chem Thermodyn. 2018;116:85–96. https://doi.org/10.1016/j.jct.2017.08.025.
59. Roy S, Guin PS, Mondal S, Ghosh S, Dolui BK. Solubility of glycine and DL-nor-valine in aqueous solutions of NaNO3 and KNO3 and measurements of transfer thermodynamics. J Mol Liq. 2016;222:313–9. https://doi.org/10.1016/j.molliq.2016.07.050.
60. Hossain A, Roy S. Solubility and solute-solvent interactions of dl -alanine and dl -serine in aqueous potassium nitrate solutions. J Mol Liq. 2018;249:1133–7. https://doi.org/10.1016/j.molliq.2017.11.104.
61. Kumar H, Singh G, Kataria R, Sharma SK. Volumetric, acoustic and infrared spectroscopic study of amino acids in aqueous solutions of pyrrolidinium based ionic liquid, 1–butyl–1–methyl pyrrolidinium bromide. J Mol Liq. 2020;303: 112592. https://doi.org/10.1016/j.molliq.2020.112592.

Publisher's Note